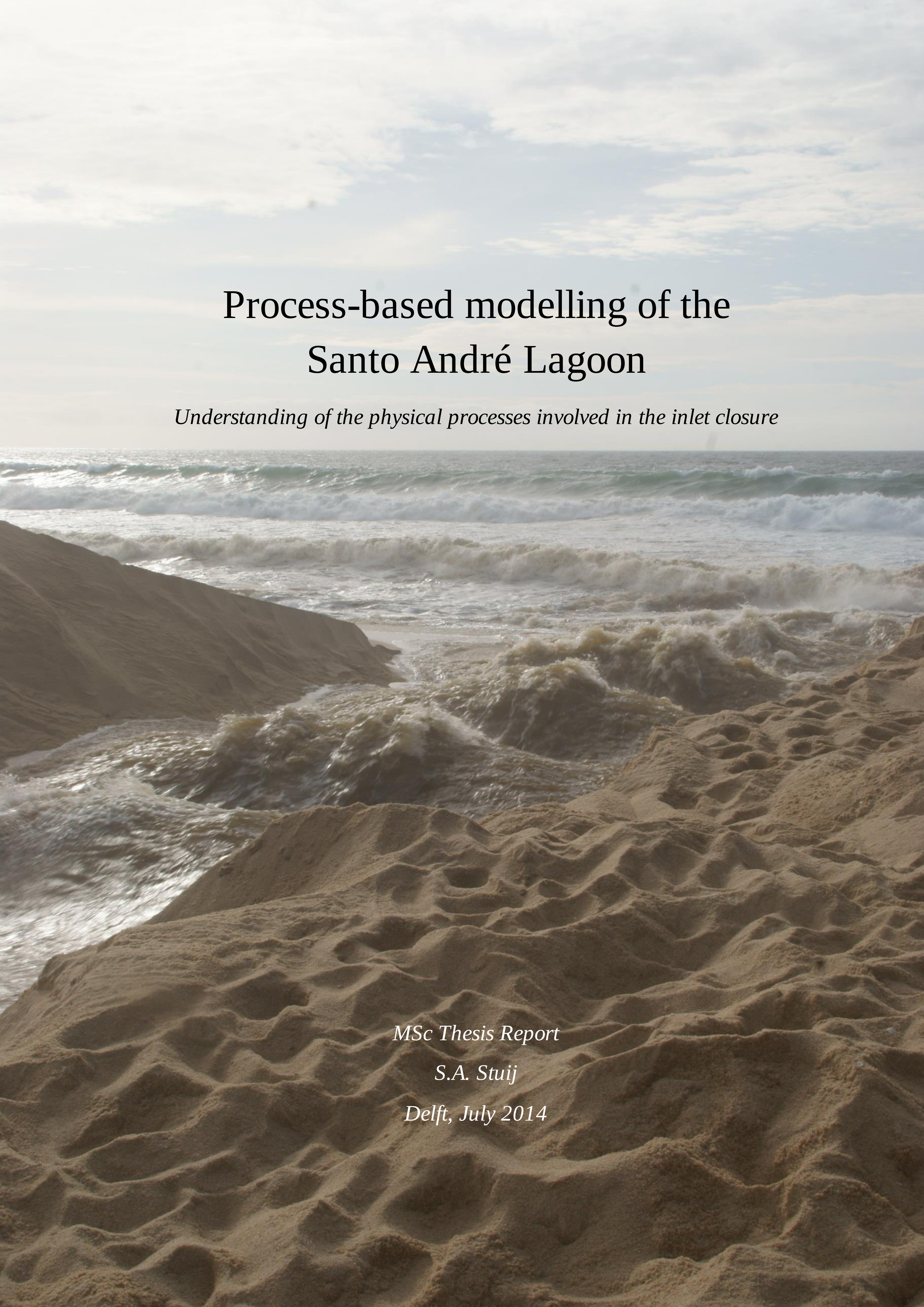

Process-based modelling of the Santo André Lagoon

Understanding of the physical processes involved in the inlet closure

MSc Thesis Report

S.A. Stuij

Delft, July 2014

Process-based modelling of the Santo André Lagoon

Understanding of the physical processes involved in the inlet closure

MSc Thesis Report

by

Sytske Aukje Stuij

Delft University of Technology
Faculty of Civil Engineering and Geoscience
Department of Hydraulic Engineering
Section Coastal Engineering

In cooperation with:

Deltares
&
Littoral Environnement et Sociétés

Committee:	Representative of:
Prof. dr. ir. M.J.F. Stive	Delft University of Technology
ir. D.J.R. Walstra	Deltares/Delft University of Technology
ir. A.A. van Rooijen	Deltares/Delft University of Technology
ir. A.P. Luijendijk	Deltares/Delft University of Technology
dr. X. Bertin	Université de La Rochelle/CNRS
dr. J.E.A. Storms	Delft University of Technology

Nec quae praeteriit, iterum revocabitur unda

Geen golf die voorbijgestroomd is kan weer teruggeroepen worden

(Ovidius, Ars Amatoria 3,63)

SUMMARY

Along the Atlantic coast of Portugal, 80 km south of Lisbon, the Santo André Lagoon is located. The Santo André Lagoon is part of a natural reserve that is officially under protection of the country. It has a rich flora and fauna and is an important place for many (protected) bird species; it is used as breeding ground, passing ground for migratory birds and for hibernating (Silveira et al., 2009). During early spring the birds are building their nests at the waterline of the lagoon.

The Santo André Lagoon is separated from the Atlantic Ocean by a sand berm. Since at least the 17th century this berm is (annually) breached artificially during lower low water spring conditions in February or March. Breaching is performed to renewal of water and to prevent the birds' nests (with eggs) from flooding. After breaching an inlet is formed and closes typically within weeks.

Understanding of the morphological development of this artificially breached inlet is of importance to maintain the nature and its biodiversity. Previous modelling gave more insight in the processes involved in the inlet closure, but did not succeed in reproducing its closure. Reasons for not being able to reproduce the inlet closure thought to be due to the fact several processes were missing and not taken into account, but may be of large importance according to Nahon et al. (2011).

In this study the main goal is to understand the physical processes involved in the closure of the artificially breached inlet. Based on measured data (data set of 2009 containing: bathymetry, wave and tidal forcing) an XBeach model is set-up to investigate the morphological development of the inlet, starting from two days after opening, until closure. Besides the general development, the influence of several processes (that were not taken into account in previous modelling) was investigated. Physical processes, such as: wave asymmetry, infragravity waves and current feedback on wave propagation (including current refraction).

Modelling of the behaviour resulted in better understanding, but did not succeed in simulating the closure. It suggests onshore transport is underestimated, because the spit formation is less than in the observations and an ebb delta is still visible. Absence of physical processes resulting in onshore transport may be a reason. Besides, still high velocities occur during the total modelling period and causes large outflow of the lagoon that may hinder the spit formation and preserving the ebb delta.

Another aspect is the tide. It seems tide is overestimated and is enlarging the inlet. During spring tide, the inlet is enlarging and the spit is decreasing more than in the observations. This is probably accompanied with the strong velocities. During neap tide the velocities are lower and a spit has started to develop, which is eroding again during spring tide. In case of high waves (H_s > 2m) approaching towards the coast with an angle of 45-60° (during spring tide), large sediment transport alongshore occur resulting in spit formation. So, large waves approaching from NNW-direction, accompanied with larger alongshore sediment transport and spring tide conditions contribute to spit formation.

Influences of the physical processes investigated have influence on the onshore transports. Increasing wave asymmetry causes more onshore transport and accretion of the coast. Infragravity waves occurring at the Santo André coast are relatively small, compared to the short waves. Comparing results, a spit is slightly better formed when the contribution of the long waves was included in the model. Therefore long waves do influence the morphological development. This better spit forming is also caused by taking into account the feedback on the wave propagation (and current refraction). Less offshore transport is visible, resulting in shallower inlet and better forming of a spit. The spit is larger (covers a larger area) and is slightly higher.

Even though the inlet is not closing in the model, with this study new insight is given in the processes involved in the closure of an artificially breached inlet and interesting approaches for further research.

ACKNOWLEDGEMENT

The ocean, the waves and the beach have always fascinated me. Chosen the right study and specialisation, finishing my master degree by doing a research in the field I am interested in most in an expiring environment of Deltares. Therefore I would like to thank a lot of people. Without them, it would not have been possible to do this research and fulfil my master degree.

In the first place, I would greatly thank my graduation committee for the inspiring meetings and discussions, for the support and guidance. Special thanks to Dirk-Jan Walstra and Arnold van Rooijen for the daily supervisions, enthusiastic support and the many hours spending in becoming familiar with XBeach. Thanks to Dano Roelvink, who is not a member of my graduation committee, but with who I had several inspiring discussions about XBeach and improving this model.

Spending almost three months in La Rochelle (France) was a great experience within this research fellowship. Many thanks to CNRS and LIENSs for giving me this opportunity. Special thanks to my supervisor, Xavier Bertin. Thank you for the interesting discussions, nice French lunches, the cycling trip at La Coubre spit, sailing trip, making me feel like home. And of course to visit the opening of the Santo André Lagoon in Portugal; it was a highlight!

The visit to Portugal would not have been such an unforgettable experience without Anabela Cruces and Vera Lopes. Thank you for this lovely day, showing me the Santo André Lagoon and telling me about its history and the breaching. It was a wonderful day, ending with a very impressive opening of the lagoon! It gave me new energy to keep on going with my research.

Thanks to my friends, for a fantastic time during our study in Delft. Besides studying, there was a lot of time for pleasant distraction. Thanks to my fellow students at Deltares for the nice coffee breaks, small talks, exchange our Matlab skills and of course for the interesting discussions about our researches and XBeach. Also thanks to the colleagues of Deltares for the nice chats, the friendly open atmosphere and for making graduation a nice time!

Last, but far from least, I want to thank my family. My parents and brother who supported me during my whole study, giving me the possibilities to do everything related to study and several side activities. But above all for the unconditionally support, especially during the last phase of my study. For always believing in me and always being there for me.

Nec quae praeteriit, iterum revocabitur unda

Geen golf die voorbijgestroomd is kan weer teruggeroepen worden – Ovidius, Ars Amatoria 3,63

Also this wave, that represents my fantastic period of studying, will flow and will never come back. But there are so many more waves approaching…

Sytske Aukje Stuij – The Hague, July 2014

CONTENTS

APPENDICES

LIST OF FIGURES

LIST OF TABLES

CHAPTER 1

Introduction

While looking to the coast all over the world, different systems can be found (e.g. barrier islands, estuaries, lagoons or tidal basins). Coastal inlets are one of these systems. They are interrupting the shorelines and connect the back-barrier bay or lagoon with the open sea. The morphology of these complex dynamic systems is constantly changing due to the influence of waves and tides. Waves and tidal currents mobilise sediment and transport it in cross-shore and along-shore direction. Transport of sediment can result in accretion and erosion of the ebb and flood deltas and the adjacent coast. Besides, sediment transport can influence the dimensions of the inlet channel; migrating, widening and deepening or closing.

Tidal inlets are of great economic and environmental importance. Sustainable management and maintaining of these inlets faces conflicting challenges. Behind the inlets in the lagoons, harbours can be situated and maintenance of open navigational routes is necessary. But the lagoons may also be important for aquaculture or recreational purpose and water renewal is essential for this. Besides, not only the inlet and the lagoon behind are important, also the stability of the adjacent coast. Often these tidal inlets experiences fast and intense morphological changes, associated with wave and tidal forces. Only in a few hours breaching of a sand berm can occur and shaping an inlet. Because of these rapid morphological changes, it is difficult to predict the behaviour of these systems.

Studies need to be performed to improve the understanding and prediction of the behaviour of tidal inlets, but it is challenging to predict with sufficient accuracy in case of morphological changes on short-time scale. Nowadays, numerical modelling is often used in studies about morphological changes. It may be a valuable tool in understanding of behaviour of inlets and the processes involved, provided that sufficient data is available. But it can also be time-consuming and not possible to make a general model for every kind of inlet. Every inlet is unique, with different influences, different processes and different conditions.

Along the Portuguese coast several inlets and lagoons can be found (e.g. mixed-energy tidal Ancão Inlet (Bertin et al., 2009c), wave-dominated Óbidos Inlet (Bertin et al., 2009a)). These coastal systems have a large ecological value and are important for a rich biodiversity. They provide natural habitats for many species (birds, fish, and shellfish). Several lagoons are breached artificially[1] every year to renewal the water and maintain the ecological environment. To open these inlets at the right time and location, with the right dimensions of the channel, knowledge and previous experiences is used. Studies and research is performed to optimise the opening and understanding the development of the inlet after breaching.

The Santo Andre Lagoon is one of the many inlets along the coast of Portugal and is the subject of this study. The lagoon is part of a natural reserve, 'Reserva Natural Lagoas de Santo André e da Sancha', and has a lot of biodiversity, especially many bird species. Like for all the inlets, maintaining the environment, ecology and providing water renewal is important. In the case of the Santo André Lagoon, the birds are valuable species and need to be preserved (Silveira et al., 2009). During the winter the water level in the lagoon rises where the birds are nesting in early spring. Some of the birds are already having eggs in February and March. In order to prevent the nests and eggs from flooding, the sand berm separating the Atlantic Ocean from the lagoon is breached. This breaching is performed at the end of winter (February/March) to prevent the water level from rising even more and flooding the nests. Since at least the 17th century this yearly breaching has been carried out (Pires et al., 2011). Comparing this inlet to others, the Santo André Lagoon closes quite rapidly. Closure of this ephemeral tidal inlet typically occurs within only weeks, comparing to months or years for other inlet closures.

1.1 Problem description

The Santo André Lagoon is part of a natural reserve with protected birds. It is of great importance to understand the behaviour of the system in order to maintain the nature and its biodiversity (Silveira et al., 2009). Different physical processes are playing an important role in the development of the inlet after artificially breaching. In order to understand the behaviour of the system, the contribution of these processes need to be studied.

Several research projects of the lagoon were already performed (e.g. Freitas et al. (2003), Cruces et al. (2006), Correia et al. (2012))[2], but the behaviour of the opening and closure of the inlet has not yet been investigated in great detail. In the scope of a research project, funded by the Portuguese National Agency for Research (PNAR), the closure of the inlet has been investigated. The PNAR allowed elaborating a database over the period during the opening and closure of 2009. This database contains bathymetric and topographic surveys, which namely resulted in six bathymetry datasets (see Figure 1.1) and water level data inside the lagoon. In Figure 1.2 a timeline corresponding to the measured bathymetry is shown to give an overview of the development of the ephemeral tidal inlet.

These data were used to study the behaviour of the inlet and its closure. The modelling for this research project was performed with the process-based modelling system MORSYS2D and gave more insight in the physical processes which could be important in order to reproduce the inlet closure (Nahon et al., 2011).

---

[1] Natural breaching can occur due to overwash during storms or due to heavy rainfall.
[2] Studies about the lagoonal water composition, geochemistry and environmental changes in the lagoon.

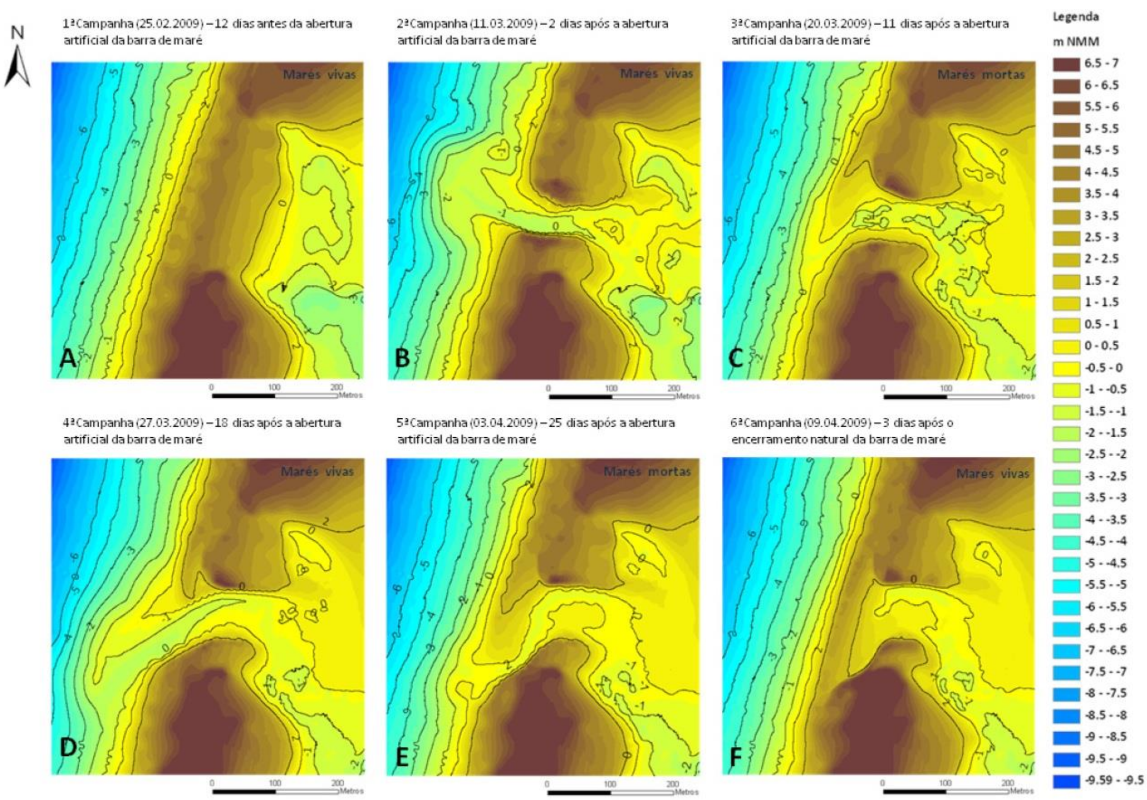

Figure 1.1 - Observed bathymetry of opening and closure in 2009

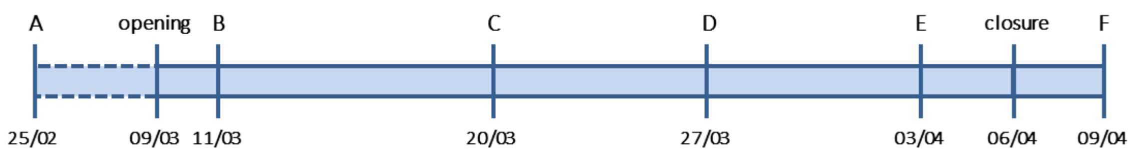

Figure 1.2 - Timeline corresponding to the measured bathymetry shown in Figure 1.1

1.2 Objective

Previous modelling gave more insight in the processes involved in closure of the inlet, but did not succeed in reproducing the closure of the inlet. Reasons for not being able in reproducing the closure thought to be due to the fact several processes were missing and not taken into account. According to Nahon et al. (2011) these processes are of importance in the inlet closure.

It is of great importance to maintain the natural reserve and its biodiversity; therefore understanding of the behaviour and development of the inlet is important. By doing so, a morphodynamic model is used, that includes the additional processes, in order to reproduce the inlet closure.

The following objective of this research can be stated:

Understanding of the physical processes involved in closure of an artificially breached inlet.

To achieve this objective, several research questions can be formulated:

- Analyse observations of measurements during opening and closure in 2009
  - How does the system develop?
  - Which physical processes are involved?
- What is the influence of the processes which were not accounted for in the MORSYS2D model?
  - Infragravity waves
  - Sediment transport associated with wave asymmetry
  - Current feedback on waves

1.3 Approach

To achieve the objective of improving the understanding of the inlet closure, this study distinguishes three phases. A conceptual model and the behaviour of the inlet system are subject in the first phase, after which the model is set up and the influence of the processes is investigated.

Phase 1: Model choice and analyse measurements

According to the previous modelling and research, some processes were not included in MORSYS2D, which could have large impact on the inlet closure. To study the closure and the influence of these processes on the inlet closure, a mophodynamic model should be used that includes these processes. Therefore the morphodynamic model XBeach is used in this study.

In this phase of the study an analysis of the evolution of the inlet system is performed by using the bathymetric surveys available of the opening and closure in 2009.

Phase 2: Set up model and calibration

In the second phase, the model is set up. The model is starting from stage B, two days after opening of the inlet. During the inlet opening the currents of 6 m/s occurred (Pires et al., 2011). These high velocities are difficult to model. Because in this study the main focus will be on the closure, this first period (opening until two days after opening) is left out. In the model set up the measured bathymetry data is used.

Input data for tide and wave conditions are gained from regional models; measurements from buoys show several gaps and are therefore not sufficient. The model described by Bertin et al. (2012) provides the tidal data and the model described by Guillaume Dodet et al. (2010) provides the wave data.

The settings gained after calibration are used for further study the development of the inlet system and the inlet closure.

Phase 3: Investigate development of inlet and influence of physical processes on closure

The key objective of this study is to investigate the inlet closure and gain knowledge of the physical processes involved. In this phase the settings gained form the calibration part are used for this. The model predictions are compared to the bathymetric surveys available over the simulated period.

Another objective is to investigate the influence of physical processes that were not taken into account in the previous modelling. In order to gain more knowledge of the contribution of these processes, simulations with and without these processes are compared. Especially the contribution on the sediment transport, velocity and bathymetry is investigated.

1.4 Thesis outline

The structure of this thesis report is based on the three different phases and starts with a description of the Santo André Lagoon, accompanied with additional theoretical background (Chapter 2). An overview and short description of previous research and previous modelling work is included in this chapter. The chapter ends with a 'conceptual model', in which the behaviour of the Santo André Lagoon system is described.

For this study the morphodynamic model XBeach is used. A short explanation of this model and the difference between MORSYS2D (which was used in previous research) is given in Chapter 3. In this chapter a short description of the implementation in XBeach of the important physical processes and parameters is given, as well as the setup of the model.

The second phase – calibration – is described in Chapter 4. After this phase the right settings for this case are obtained in order to investigate the influence of the physical processes. Investigation of the development of the inlet and the influences of physical processes on its closure are described and shown in Chapter 5, where the results of these simulations and investigations will be discussed as well. This study will be completed with conclusions and recommendations in Chapter 6.

CHAPTER 2

Santo André Lagoon

Santo André Lagoon, or 'Lagoa de Santo André' as it is known in Portugal; a description of the lagoon and the area is given in this chapter, accompanied with general knowledge of the hydrodynamics and morphology (section 2.1-2.3). Previous research and modelling on The Santo André Lagoon is performed, an overview of this is given in section 2.4. Extra analysis of the available data is performed and shown in section 2.5. An explanation and expectation of the behaviour of the inlet system is the last topic described (section 2.6).

2.1 Area description

Along the Alentejo coast of Portugal, between the mouth of the Sado close to Setúbal and Sines, several wide beaches and dunes can be found. Several (little) lakes and lagoons are hidden behind these sand hills. At the southern half of the Tróia-Sines littoral arc, 80 km south of Lisbon, the largest lagoon is situated; the Santo André Lagoon (Figure 2.1). Its maximum dimensions reach 2 by 1.5 km in respectively the N-S and W-E direction and is separated from the Atlantic Ocean with a sand barrier of around 5 km length, N15°E orientated. The barrier is formed by an active beach-foredune system including numerous washovers in the northern tip, where the height is less and around 4 meter. In the south part of the barrier, the beach and foredune weld and lean against an older, robust and vegetated aeolian ridge (Cruces et al., 2009).

Since 2000 the lagoon is part of the natural reserve 'Reserva Natural das Lagoas de Santo André e da Sancha'. The reserve is one of the areas in Portugal which is officially under protection of the country. It has a rich flora and fauna and is an important place for many (protected) bird species; it is used as breeding ground, passing ground for migratory birds and for hibernating.

At least since the 17^{th} century, the sand barrier is artificially breached regularly (annually) during lower low water spring conditions to maintain the water quality (promoting water exchange, prevents eutrophication and drain the alluvial deposits, reclaimed for agriculture (Cruces et al., 2009). Besides the renewal of water, it is of great importance for the many bird species to breach the berm and lower the lagoonal water level. The birds are building their nests close to the waterline in early February and March, when the water level is high and still increasing. Only lowering of the lagoonal water level can prevent the nests (with eggs) from flooding. Therefore breaching of the barrier is usually performed in February or March[3].

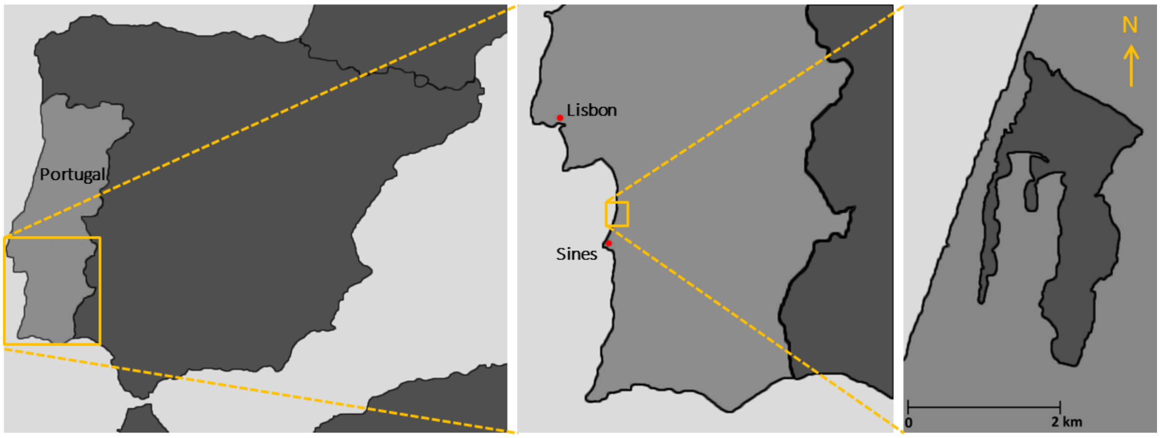

Figure 2.1 - Overview of the location of the Santo André Lagoon in Portugal

The barrier is not only breached artificially, but it also occasionally breaches during storms (Cruces et al., 2009) or after heavy rainfall, when the water level is too high and an overflow over de barrier induces a breach. In this case, the barrier breaches in the northern tip, where the height of the barrier is low. In 1997 the last breaching by storm occurred. Since then only artificially breaching occurred (Cruces, 2014).

During the period in which the inlet is closed, the tide cannot influence the lagoonal water level and other aspects control the water level. Fresh water reaches the surface of the lagoon directly by precipitation or through fluvial input. Salt water can enter the lagoon due to overwash, during high wave events. When this happens, it mainly occurs at the location of the former channel in the northern tip of the berm, where the height of the berm is lower. These aspects control the water level due to their input and evaporation will control it by lowering of the water level.

Every year when the winter has ended, an inlet channel is excavated. At low water during spring tide, when the head difference between the lagoonal water level and the water level of the ocean has its maximum, the inlet is breached (Pires et al., 2011). After breaching, the ephemeral tidal inlet typically closes within weeks.

There are no rules or restrictions for excavating the channel. The operator of the excavator decides the dimensions of the channel, but these are of about 20 m in width and 1 m in depth and the excavated sand is dumped just next to the channel.

2.2 Hydrodynamics

The adjacent coast of the Santo André Lagoon experiences a meso-tidal regime and a high energetic wave climate. These factors have influence on the sediment transport and are of importance in the development of the inlet, resulting in closure. In the following sections the hydrodynamics and morphology will be described for the inlet of the Santo André Lagoon.

[3] In some years breaching was performed in April.

2.2.1 Tide

Tidal waves are the longest of oceanic waves, which can only be observed as fall and rise (ebb and flood) of the sea level and is the result of the gravitational attraction of the earth and the moon and of the earth and the sun. Worldwide shorelines are not exposed to the same tidal regime, not the same period of falling and rising water. According to Ranasinghe and Pattiaratchi (2000) the most common tidal regime in the world is a semi-diurnal regime.

Besides the differences in period of the falling and rising water, also a distinction of the tidal ranges can be made. Three tidal regimes can be distinguished: micro-, meso- and macro-tidal. These regimes have a mean spring tidal range of respectively <2m, 2-4m and >2m.

Along the Portuguese coast a semi-diurnal regime is appearing and it experiences a meso-tidal regime. The average tidal ranges in the region of the Santo André Lagoon are 1.2 m during neap tides and 2.9 m for spring tides. Higher tidal ranges can occur, with a range of 3.6 m, which correspond to a maximum high-tide level of about 2 m above MSL (Bezerra et al., 2011).

Tidal inlet

Tide is a complex process acting on the coast. It is even more interesting and complex when involved in an inlet. After (artificially) breaching of the sand berm high velocities occur and tide will flow in and out, which cause a strong sediment exchange between the lagoon and the ocean.This exchange leads to formation of tidal deltas, extensive sand deposits. During ebb the velocities are directed to the sea and therefore an ebb delta is formed in front of the inlet at the sea side of the inlet. During flood the opposite occurs and a flood delta is formed in front of the inlet, but at the lagoonal side of the inlet. Depending on the tidal ranges, the tidal deltas are well-developed. Boothroyd et al. (1985) discerned several elements for the ebb and flood tidal delta, which can be found in Appendix A.

2.2.2 Waves

Waves are generated by winds (during storms) offshore at the oceans and propagate to the coast. The waves travel in wave groups with higher and smaller waves and propagate to the coast with a group velocity or phase speed (c_g), which is a function of the wave length. Besides, the waves transport energy, $P_{energy} = Ec_g$. In deeper water it means that waves with a larger length travel faster. At a certain moment the waves start to be affected by the bottom and slow down. That is when the water depth becomes less than about half the wave length and the group velocity equals the wave velocity. *Shoaling* occurs (in the *shoaling zone*) as the waves slow down, causing concentration of wave energy, which result in an increase in wave height, $E = 1/8\rho g H^2$. Propagating further to the coast, the waves are becoming higher and steeper and so more unstable and start breaking (in the breaker zone) when the particle velocity exceeds the velocity of the wave crest.

Together with the wave groups a bound long wave is travelling with the wave group. The bound long wave has the length and the frequency of the group and travels with the wave group velocity. When the waves start breaking, the bound long waves are released as free waves (Longuet-Higgins & Stewart, 1962)and propagate further to the shore. There the free long waves will be reflected and propagate back offshore or the will be trapped in the surf zone.

While waves are propagating they transport energy, but also momentum. The transportation of wave induced momentum is known as radiation stresses, which have a great contribution in the alongshore transport of sediment. Variations in the radiation stresses result in several currents (e.g. alongshore, rip and undertow), which are important for the transport of sediment.

High and low frequency waves

Wind generated gravity waves have different frequencies. In this case a distinction of two is made: *high* and *low* frequency waves. Both are important in the supply of energy to the coastal system and thus important for the sediment transport.

High frequency waves, generated by wind, are also called short waves. Usually they have a period between 0.25 – 30 s and their size depends on the wind (duration and velocity), fetch and the water depth. From the area of generation they can travel large distances and will transform into longer, faster, lower and more regular 'swell' due to frequency dispersion. Short waves travel in groups, as explained before, which is an effect of the frequency dispersion.

Low frequency waves have larger period than the high frequency waves (period of 30 s – 5 min) and are smaller. As explained before, the short waves travel in groups of higher and smaller waves. This means that the energy and radiation stress is varying as well, causing the largest depression under the highest waves.

Due to these variations a bound long wave is formed, which travels with the wave group speed and has the length and the frequency of the wave group. Therefore the low frequency wave is considered bound to the short wave group (Longuet-Higgins & Stewart, 1962).

In the situation of a complete bound long wave, there is a phase shift of 180 degrees between the low frequency waves and the short wave envelope. Meaning that maximum bound long wave values correspond to minimum short wave values and vice versa. This complete bound long wave phenomenon is not exactly the case in reality. The correlation between the bound long wave and the short wave groups is smaller, so more irregular. But this will change into a positive correlation, when the waves propagate further to the shore and enter the surf zone. The bound long wave is no longer travelling with the wave group velocity, short waves will break and the bound long wave is released and becomes a free long wave. The free long wave propagates further to the coast where it will be reflected and propagate out of the surf zone or the wave will be trapped in the surf zone.

Along the Portuguese coast high energetic wave conditions occur. The waves are predominantly from North-West and West direction, representing respectively 77.3% and 20% of the time, inducing a southward-directed littoral drift (Bezerra et al. (2011); Costa et al. (2001)). The mean offshore wave conditions are quantified by a significant wave height of about 1.7 meter. (Significant wave height of 1-2 meter is represented 49% of the time.) The average peak period is 10.8 s, where 60% is covered by a peak period between 9 and 13 s. Extreme conditions with a significant wave height of >5 m and a peak period of >15 s represent respectively 0.6% and 6.1% (NW-direction) and 1.7% and 7.9% (W-direction) annually (Costa et al., 2001).

Wave asymmetry and skewness

Wave propagating is not linear, but waves are irregular and show nonlinearities/non-linear interactions. When waves are propagating towards the shore, they become higher, steeper and thus more asymmetric until they start breaking. As said in the previous part, the process of increasing of the wave height is called *shoaling*. This process is characterized by *skewness* and *asymmetry*. Both processes are crucial in determining the magnitude of the wave-induced sediment transport (Bosboom & Stive, 2012).

In case of wave *skewness* the wave crest is gradually peaking and the wave trough is flattening, which can be observed in shallow water. According to this wave shape, the velocities under the crest are higher (onshore directed) than the velocities under the trough (offshore directed) (Holthuijsen, 2007). Velocity causes mobilisation of the sediment. Since the velocities under the crest are higher, more sediment is mobilised and thus causes a net onshore sediment transport. Skewness can cause offshore transport due to phase-lag effects; the sediment is mobilised by the velocities under the wave crest and is transported by the velocities of the following trough. This results in a net offshore directed sediment transport (Grasso et al., 2011).

The second process is wave *asymmetry*, where the wave results in a pitched-forward shape, also called a saw-tooth shape. The waves become steeper which results in a steep wave front and a smooth wave back. This shape is the result of a difference in velocity. In shallow water the wave crest moves faster than the wave trough, which can be shown by the propagation speed of non-linear shallow water waves: $c_{crest} = \sqrt{g(h+a)}$ and $c_{trough} = \sqrt{g(h-a)}$, in which a is the amplitude (Bosboom & Stive, 2012). The accelerations in the wave crest are higher and therefore causing a net onshore directed sediment transport as explained above.

Wave skewness and wave asymmetry are therefore of great importance in wave-induced sediment transport.

For the waves approaching the coast of the Santo André Lagoon, there is no information about the wave skewness and wave asymmetry.

2.3 Sediment transport & morphology

Movement of sediments is covered by morphodynamics and explains the changes of a coastline. Still the processes involved in sediment transport are not fully understood, although many researches are performed.

Sediment transport can be divided in cross-shore transport and in longshore transport. Cross-shore transport is the transport of sediment in onshore or offshore direction. Longshore sediment is the transport along the coastline. Sediment is stirred up by waves and then transported by currents (caused by oblique incident waves) or by tidal currents. The amount of sediment transported (alongshore) can be visualised as a function of the wave angle at deep water, so-called (S,φ)-curve. As can be seen in Figure 2.2, there is a maximum sediment transport (alongshore), when the waves approaching the coast with an angle (according to shore normal) of about 45°. An angle of 0° implies normally incident waves and an angle of nearly 90° implies a wave approaching nearly parallel to the coast, which reflects hardly any wave energy towards the coast. For waves propagate with a negative angle (according to shore normal) have the same sediment transport as waves with the same positive angle, but have a sediment transport in the opposite direction.

The coastline adjacent of the Santo André Lagoon is N15°E orientated and the waves are predominantly coming from North-West and West direction. This means that in case of NW-directed waves, the waves are approaching the coast with an angle of 30° and -15° in case of W-directed waves. This is also indicated in (S,φ)-curve in Figure 2.2.

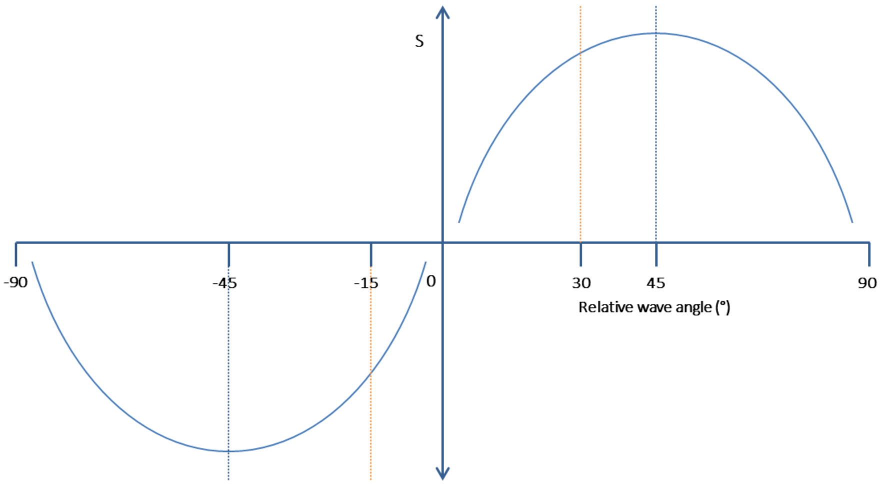

Figure 2.2 – Simplification of the longshore transport as a function of the wave angle (deep water), with indications of the predominant wave directions (orange)

A distinction in bed load and suspended load transport can also be made. The sum of these transports is the total sediment transport: $S_t = S_b + S_s$. Bed load transport is the transport of sediment in a thin layer close to the bed. The sediment is more or less in continuous contact with the bed. In contrast to bed load, suspended load has no contact with the bed and contains the transport of sediment suspended in the water column. The sediment transport can be calculated by several transport formulas, e.g. Soulsby – Van Rijn (Soulsby, 1997) and Van Rijn – Van Thiel (Van Thiel de Vries, 2009).

The adjacent shore of the Santo André Lagoon has a steep beach, with a slope of 1:10 and the beach profile does not experience significant erosion or accretion during mild wave conditions. For the sediment grain diameter samples are used to define D50 of 1.15 mm and D90 of 1.18 mm (Nahon et al., 2011).

2.4 Previous Research & Modelling

Since at least the 17th century the sand barrier is breached artificially, but only since 1998 some monitoring has been done. During this year monitoring of the lagoonal water level has been performed, in association with field geomorphological observations and topographic surveying (Cruces 2009).

Several studies about the lagoon are performed (e.g. about the water quality, biodiversity etc.), but less detailed research is performed in understanding of the behaviour of the inlet and its closure. The latter is of importance in understanding the duration of the opening for renewal of the lagoonal water and lowering of the water level.

Since 1998 the lagoonal water level has been monitored, started just before the inlet opening and monitoring during the period of an open inlet until two days after closure. In 2009 the water level was measured with a pressure transducer and recorded the level every 10 minutes. Tide and wave data is yielded from the Sines tide gauge records and from the deep-water Sines buoy between 1998 and 2009.

Other measurements are performed in the scope of a research project funded by the Portuguese National Agency for Research (PNAR). At six different moments in time, the bathymetry is measured (shown in Figure 1.1). The topographic information was obtained from a combination of a kinematic Differential Global Positioning System (RTK-DGPS) and echo-sounding. This was connected to a navigational interface running hydrographic survey software (HYPACK® 2008, Coastal Oceanography Inc.) covering the inlet main channel, and flood delta, when navigable. To cover the non-navigable areas total stations (Zeiss RE50 and Leica TC4 700) and RTK-DGPS (Leica GPS900) were used.

Besides the bathymetry, velocity currents in the inlet were also measured during this project. The velocity was measured during the first 26 hours after the inlet opening with floats deployed in the centre of the channel, giving a measurement every half hour. Currents are peaking at 6 m/s during the first (prolonged) ebb and 2m/s during the first flood (Pires et al., 2011).

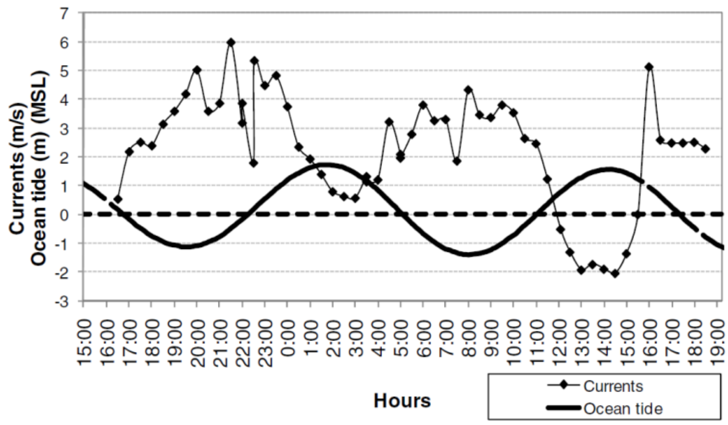

Figure 2.3 - Velocity currents at the inlet and oceanic tide on March 9 and 10, 2009 (Pires et al., 2011)

2.4.1 Previous Research

These measurements are used for several researches to understand the development of the inlet. Previous researches are performed by Cruces et al. (2009), Bezerra et al. (2011) and Pires et al. (2011). In these researches the development and the lifespan of the inlet have the main focus.

Evolution

Based on the observations (shown in Figure 1.1) the evolution of the inlet until closure can be divided in several stages. After the artificially breaching of the sand berm, prolonged ebb occurred, forming a linear V-shaped channel. During this first ebb, high velocities causing erosion of the inlet and sediment is flushed out and an ebb delta is formed. After two days (B in Figure 1.1) the channel has deepened up to -1.5 m MSL, in the meantime the outflow is taken over by the tide and a flood delta started to develop. During the second period (from B to C, 11 days after opening), the formed ebb delta is migrating shoreward and resulted in spit formation (+0 m MSL) and the direction of the inlet channel is changed in southward direction. The channel is increasing in width and became flat-floored with a depth of about -1m MSL during the same period. During the next week (C to D, 18 days after opening) the formed spit is moving offshore and is lying below MSL. After another week (D to E, 25 after opening) the spit is migrated onshore again with a height above MSL. The channel is meandering and it started silting up. Several days later the spit is moving further onshore, becoming a berm and starting to block the inlet. During the last stage (E-F) the inlet closed rapidly due to accretion of the berm to an equilibrium height. Months after the closure the inlet, the berm is not accreted significant until winter, when the waves cause a new accretion pulse for the berm and of which the crest is increasing up to +3 m MSL in December 2009 and +4 m MSL in January 2010.

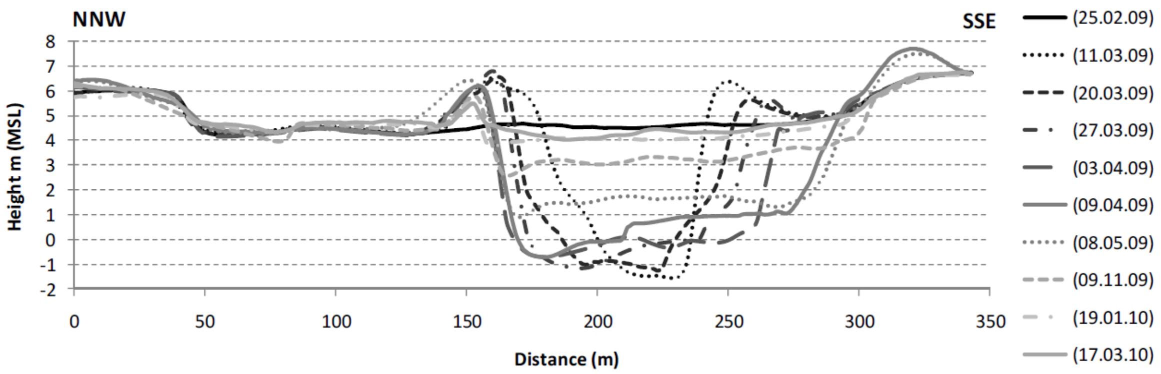

Figure 2.4 - Time series of the inlet's cross-section (Pires et al., 2011)

So in fact, the evolution is characterised by ebb dominance (strong ebb currents, outflow of the lagoon into the sea), which cause scouring of the inlet channel and forming an ebb delta in the first days after the breaching. In the latter part, the tide is acting on the channel (more similar current velocities, ebb and flood tending towards equilibrium) and causes meandering of the channel, forming a flood delta and an offshore spit. Despite these morphological changes, the inlet itself is not migrating noticeably in alongshore direction.

Lifespan

From the monitored lagoonal water level, recorded between 1998 and 2009, six factors are found which influences the lifespan of the ephemeral inlet (Cruces et al., 2009):

1) Initial Lagoonal Water Level (ILWL)
2) Hydraulic head between lagoon and ocean (magnitude + persistence) during the first tidal cycle
3) Magnitude of first lagoonal prism flushed out after opening
4) Inlet section (shape and dimensions)
5) Initial size and location of ebb delta
6) Wave and tide regime following the inlet opening

It is founded that the ILWL is the most important of the six factors in the study of Cruces et al. (2009). It is the only variable independent of oceanographic forcing and is essentially modulated by rainfall and morphology of the lagoonal basin, defining an initial condition, which varies every year. Besides the ILWL controls the duration of the ebb period, directly after breaching, and therefore the dimension of the inlet, dimensions and location of the ebb delta, which result in controlling the duration of the inlet activity. A significant correlation between the ILWL and the lifespan of the inlet was found in the same study. A clear correlation between inlet closure and wave and tide conditions was not found, although the inlet closure occurred preferably during neap tide cycles.

Tidal prism

In the study of Pires et al. (2011) the correlation between the minimum cross sectional area below MSL of an inlet gorge and the corresponding spring tidal prism of the Santo André Lagoon is determined. Using the measured bathymetry the cross sectional area and tidal prism is estimated with the equations presented by O'Brien (1969) and Jarrett (1976). The results are plotted, together with data of O'Brien and Jarrett, shown in Figure 2.5. Santo André's tidal prism is higher than expected considering the observed minimum cross sectional area. According to the study of Pires et al. (2011), it is probably the cause of a shallow inlet of which most of the channel gorge develops above MSL. This is in contrast with the large systems studied by O'Brien and Jarrett, where most of the cross sectional area develops below MSL.

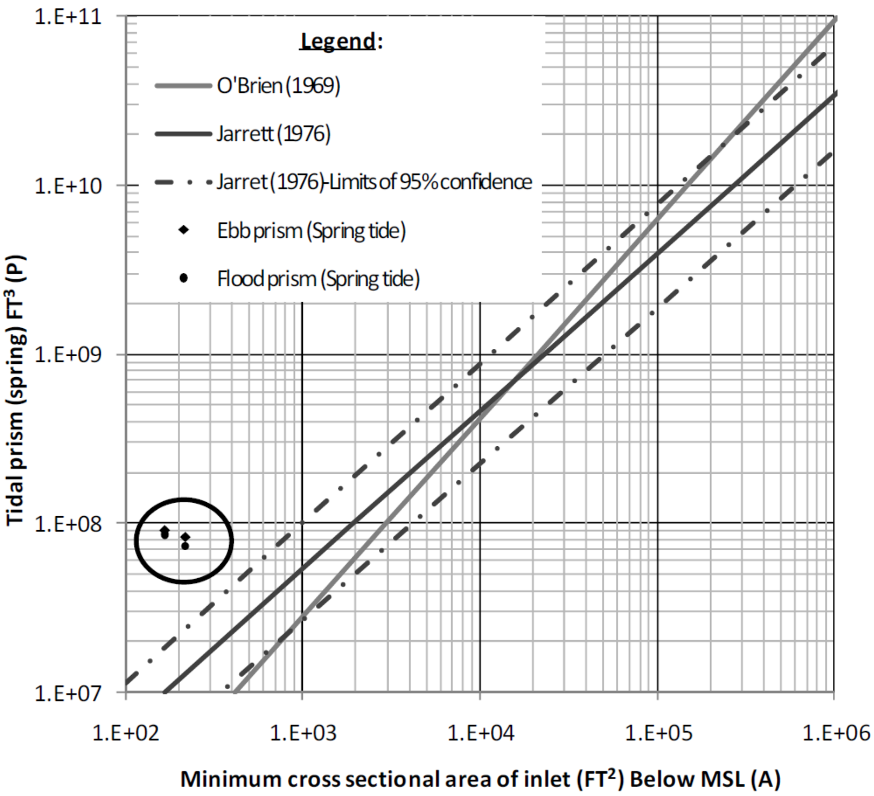

Figure 2.5 – Relationship between tidal prism and cross sectional area of the Santo André Lagoon, compared with the empirical approaches of O'Brien (1969) and Jarrett (1979).

Previous Modelling

Morphodynamic models can be a tool in understanding the behaviour of coastal systems. Nahon et al. (2011) used the model MORSYS2D to gain more insight in the important processes involved in the evolution and closure of the Santo André Lagoon. A short description of MORSYS2D can be found in Appendix B. The model for this part of the Portuguese coast is forced by results of regional wave (Guillaume Dodet et al., 2010) and tide (Fortunato et al., 2002) models. For this study, some 'new' processes were implemented in MORSYS2D, which could play a role in the development and closure of the inlet:

- Hydraulic jumps – associated with extremely strong currents which occur in the first hours after the opening of the inlet – were taken into account by applying a correction to the drag coefficient.
- Avalanching processes, which are responsible for the rapid enlargement of the tidal inlet, are represented using a numerical filter that prevents a user-specified, spatially-varying bottom, slope to be exceeded.

With the model MORSYS2D it is possible to simulate the first days after opening of the Santo André inlet. But after these days the model shows a bathymetry which is completely different than the observed bathymetry (Figure 2.6). Only the water level in the lagoon corresponds with the measured water level (Figure 2.7) until 25 days after opening. There are several causes for not reproducing the closure of the inlet. Limitations (i.e. lack of implementation of physical processes) in modelling are discussed by Nahon et al. (2011), associated with the lack of data.

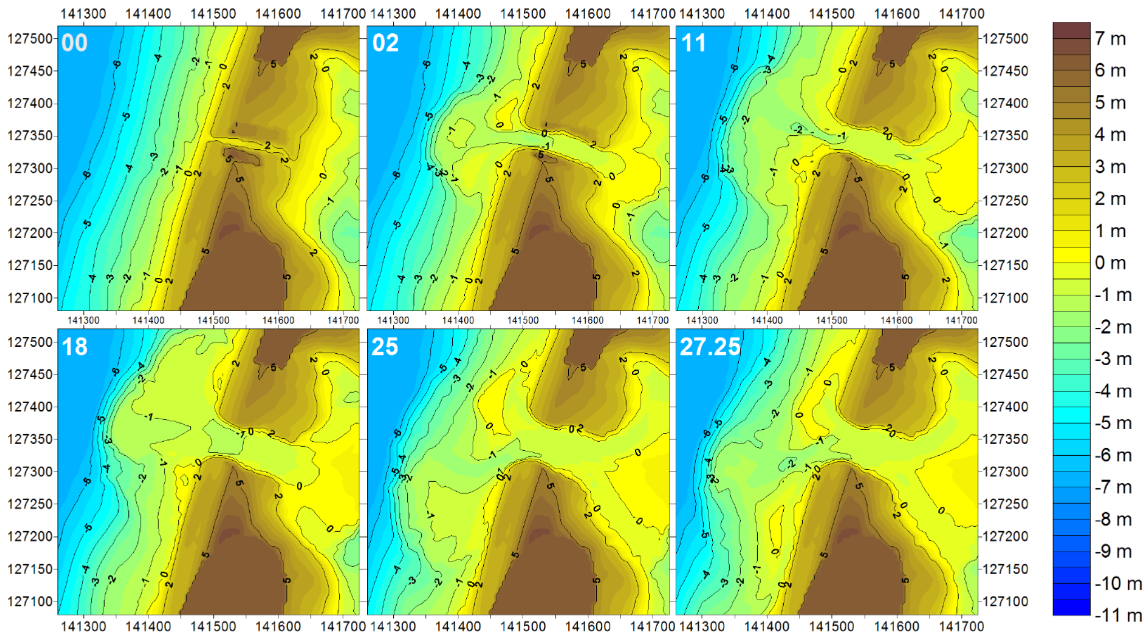

Figure 2.6 - Simulated morphological evolution of the Santo André Lagoon Inlet. The simulated time, in days, is indicated in white in the left upper corner of each view (Nahon et al., 2011)

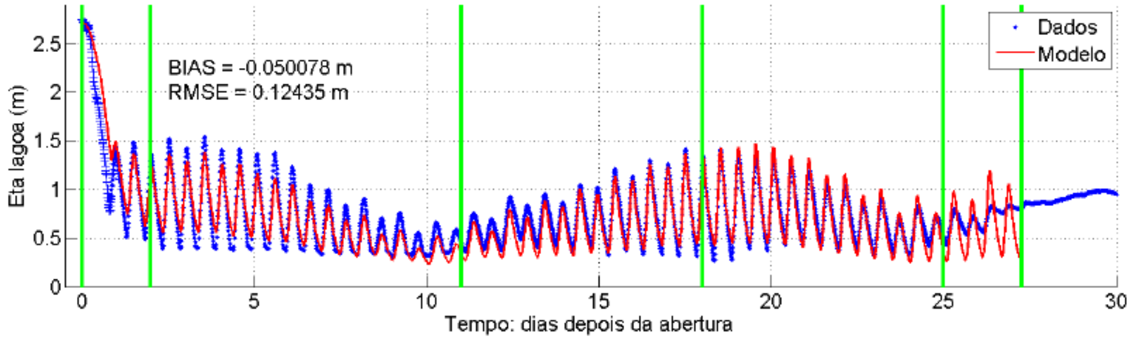

Figure 2.7 - Validation of MORSYS2D system: comparison between simulated and measured water levels inside the lagoon. The green lines indicate bathymetric output in Figure 2.6. (Nahon et al., 2011)

These discussed limitations are the following:

1) Clogging of the inlet channel was underestimated and it was not able to reproduce the damping of the tidal range inside the lagoon.

2) It is also likely that the closure of the mouth is partially associated with the cross-shore sediment transport, which displaces the ebb delta towards the land, filling the mouth. Because of some simplifications in the model, with regard to the cross-shore transport, it limits the correct reproduction of this process. Some mechanisms were not considered:

- The effect of infra gravity waves (see also Roelvink et al. (2009))
- The transport associated with wave asymmetry (see also Hoefel and Elgar (2003))
- Blocking of waves by ebb currents (see also Chawla and Kirby (2002); Guillaume Dodet et al. (2013))

3) Comparing the measured and simulated bathymetries, it suggests that transports in the swash zone are important. Contribution of swash is not included in the model, but it could have an important role in the growth and extension of the spit.

If the hypotheses above are correct, these processes should be implemented in order to close the inlet.

2.5 Further analysis on data 2009

In previous studies several analyses are performed. In Bezerra et al. (2011) an analysis for the volume differences in the inlet is performed. In this study a small analysis on the volume changes is performed, involving the ebb delta as well, which was not included by Bezerra et al. (2011).

Volumes

In order to understand the sedimentation and erosion of the system, a better look to the volume of the different part is necessary. The system is divided in three different areas (Figure 2.8):

- Ebb delta & spit
- Inlet
- Lagoon

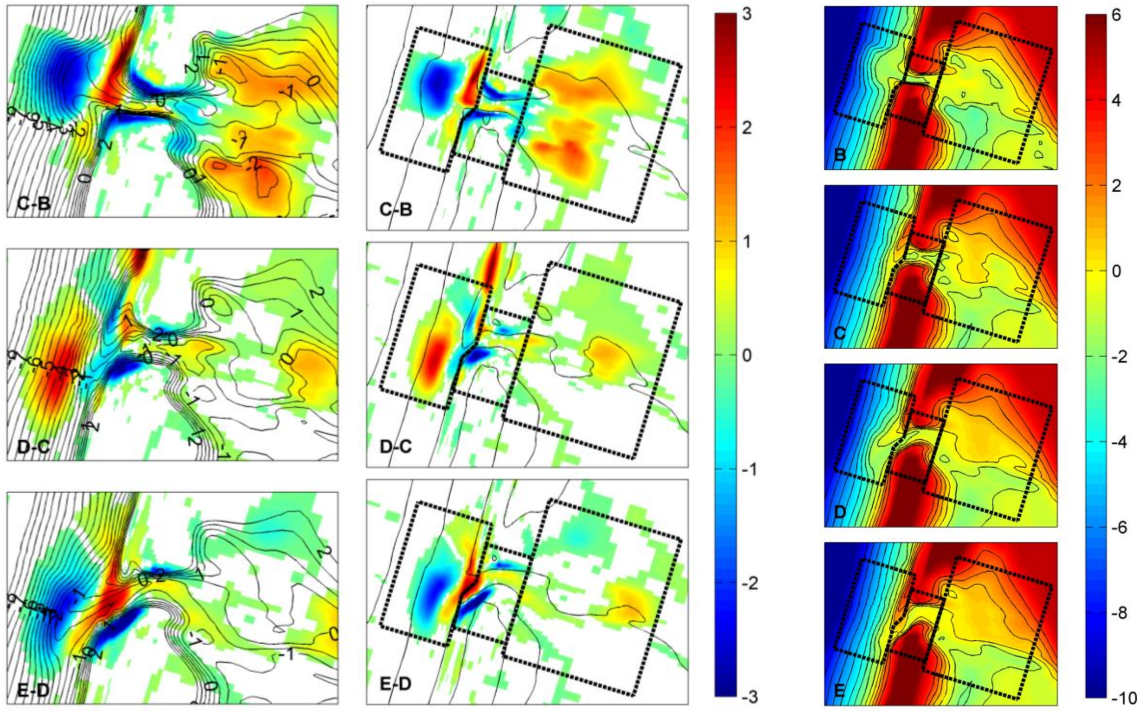

Figure 2.8 - Sedimentation (red) and erosion (blue), contour lines correspond to the 'initial' bathymetry (i.e. upper figure shows sedimentation and erosion in the period from B to C and has the contour lines of the bathymetry in stage B). In the middle figure the indication of the different areas in the sedimentation/erosion figures. In the right figure the indication of the different areas in the bathymetry [m] MSL.

In the first area large erosion and sedimentation can be seen during the period. To quantify and visualise what is happening exactly and how the ebb delta and spit are developing, different ranges in depth are defined in order to calculate the volumes.

Some remarks need to be made. For every period the same areas are used to calculate the volume, but not in every stage all the subparts are present in the larger parts. It is difficult to define a general area for the ebb delta, spit and the inlet, because the locations of these subareas are changing and overlapping a bit. For example, in the period from D to E, Figure 2.8 middle and right figure), the boundary of the first and second area crosses the spit forming (the accretion, red in the middle figure). A distortion in this period is expected to see in the volume trend-line for the spit forming, which is larger (according to Figure 2.8, left and middle figure) than visible in the trend-line. For the inlet there is expected to be a small distortion as well. In order to visualise these distortions and to get a more detailed view of the volumes changes, the volumes are calculated for different depth ranges.

As can be seen in Figure 2.8, stage B and C-B respectively, the ebb delta ends at -7.5m depth. Therefore the range to calculate the volume of the ebb delta will be between -7.5 m depth and -0.5 m depth. The spit is defined as the area between a depth of -0.5 m and 3 m. Deeper than -7.5 m and higher than 3 m are two other parts in this defined area. For the inlet there are two different parts defined. The inlet channel is defined as deeper than -0.5 m and the dunes of the inlet are defined as higher than -0.5 m. The lagoon is only one area.

Based on the defined ranges the volumes are calculated for each area and subpart for every bathymetry. In Figure 2.9 these volumes are plotted for every stage (i.e. the dots represent the volumes for every measured bathymetry).

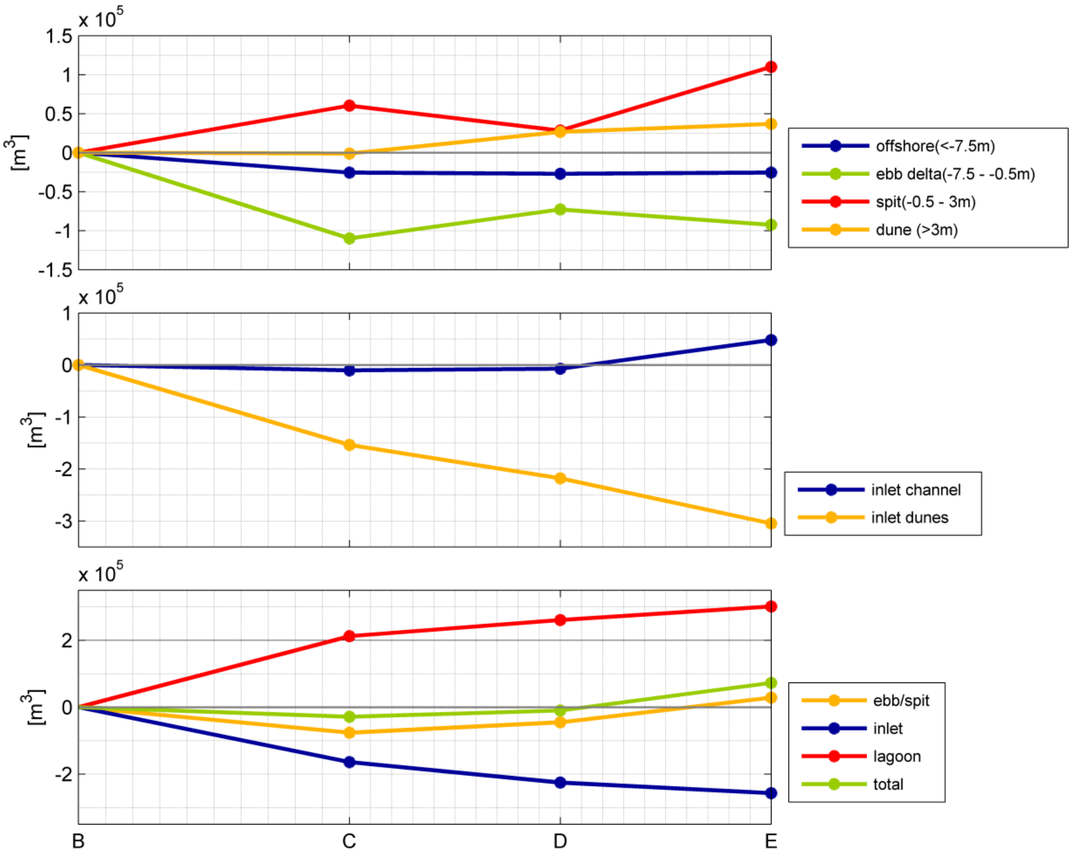

Figure 2.9 - Volumes from measured data. Ebb delta and spit area (up), inlet (middle) and total of each area (bottom).

Comparing Figure 2.9 with the bathymetry and sedimentation and erosion figures (Figure 2.8), the spit is growing in the first period (B-C), which is also noticeable in Figure 2.8, where a red spot is visible in the upper plot. In the same period the ebb delta is eroding almost with a double volume (compared to the volume of the spit). Offshore some erosion is visible and the dunes are not changing. In the second period (C-D), the spit is eroding a little and the ebb delta is accreting. Offshore there are no changes anymore and the dunes are accreting a little. In the last period (D-E) the spit is growing and the ebb delta is eroding again, which clarifies the red and blue spots in Figure 2.8.

In the middle plot of Figure 2.9 the two different ranges of the inlet area are shown. The inlet channel is eroding a little in the first periods and accretes in the last period, which indicates silting up of the channel. Whereas the dunes in the inlet area are extremely eroding, this explains the widening of the inlet channel.

The total volume changes of the three areas are shown in the lower plot of Figure 2.9. The lagoon and its flood delta is in the first period fed with a lot of sediment and after that, it is still accreting a bit. The opposite happens with the inlet; this is eroding a lot. As shown in the upper plot, there are large volume changes within the different ranges, but the total volume change of the ebb/spit area does not shown the same large differences.

In order to improve the understanding of the volume changes in the system, the following schematised blocks are shown (Figure 2.10). As can be seen in the left figure, the total volume change during this period is negative, which means that besides a lot of eroded sediment from the ebb delta and inlet is flowing into the lagoon, causing accretion of the flood delta, some sediment is also going out of this observed area. This sediment could be transported alongshore or in offshore direction. During the second period (middle figure) there is more accretion in the system. The lagoon is still accreting (as is also noticed in Figure 2.9), with probably some sediment from the inlet. But not all the eroded sediment from the inlet is flowing in the lagoon; some is flowing out, probably forming the ebb delta or spit. It is also possible that there is a significant alongshore transport and the sediment from the inlet is transported north- or southward. In the last period there is even more accretion, which indicates the growing spit and almost closure of the inlet, probably caused by alongshore transport.

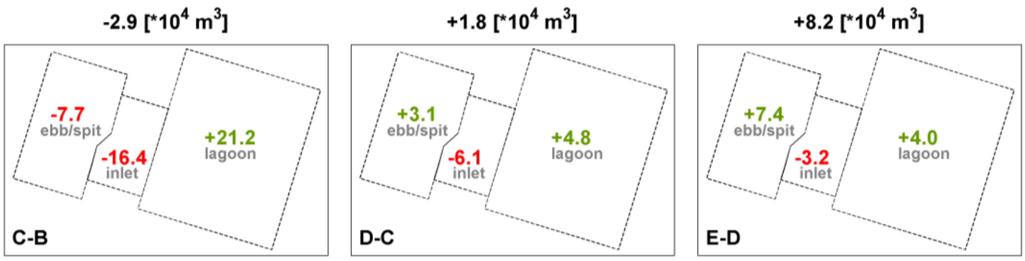

Figure 2.10 - Schematic overview of the volume changes, on top the volume change of the total system.

As in Figure 2.9 can be seen, the volume changes in the ebb delta-spit area are large, therefore a detailed overview is given in Table 2.1.

[*10^4 m^3]	*B-C*	*C-D*	*D-E*
Offshore	-2.6	-0.1	+0.1
Ebb delta	**-11.0**	+3.7	**-2.0**
Spit	+6.0	**-3.2**	+8.2
Dunes	-0.1	+2.8	+1.0

Table 2.1 – Overview volume changes ebb delta/ spit area

It seemed that the ebb delta was moving onshore and becoming the spit during the first period. According to these volume changes (i.e. the volume of the ebb delta and spit is not the same), this hypothesis is not true. Probably some of the ebb delta is moving onshore, but not totally. The remnant might be transported alongshore or more offshore. During the other periods, this can be concluded as well. The area is not in an equilibrium, therefore some alongshore movements are expected.

2.6 Conceptual model

Every year the Santo André Lagoon is artificially breached to prevent the bird's nests from flooding and to promote water renewal. After breaching, the excavated inlet channel is enlarging, but closes typically within weeks. Based on previous research and existing theory, the morphological development of the inlet of the Santo André Lagoon can be described as follows.

The beach profile adjacent to the inlet is relatively steep, with a slope of about 1:10 and relatively coarse sediment with a median grain diameter of 1.15 mm and D90 of 1.18 mm (Nahon et al., 2011). For these kinds of steep coarse-grained beaches, the short waves are relatively more important than in case of beaches with more gentle slopes. Therefore short waves processes, such as wave skewness, asymmetry and swash may play an important role in the morphological development of the beach.

The Santo André system is a closed beach system. Only a short period (several weeks) a year, the system is an open system, interrupted by an inlet, developed after artificially breaching of the Santo André Lagoon.

A tidal inlet is a dynamic system where factors such as; tidal currents, tidal prism, inlet's cross-sectional area and sediment transport are important for its stability. Escoffier (1940) was the first to study the stability of the cross-sectional area of an inlet and defined a model, the closure curve (Figure 2.11). In which the maximum velocity curve is plotted versus the cross-sectional inlet area. A second line is plotted, representing the equilibrium velocity to maintain an equilibrium flow area. Escoffier proposed this constant critical velocity of around 1 m/s. The exact value of this equilibrium value depends on sediment diameter (Van de Kreeke (1992)). The curve has two intersections with the equilibrium velocity (B and D). These two points represent an unstable (B) and stable equilibrium (D), which divide the curve in three sections. If an inlet is between the points A and B, the inlet channel is too small, the friction too high to maintain itself and velocities decrease until the inlet closes. When the inlet is right of point B, erosion takes place until point D (stable equilibrium) is reached. Lastly, if the inlet channel is on section D-E of the curve, the cross-sectional area becomes smaller accompanied with an increasing velocity. Sedimentation of the inlet channel continues until point D is reached (Seabergh, 2006).

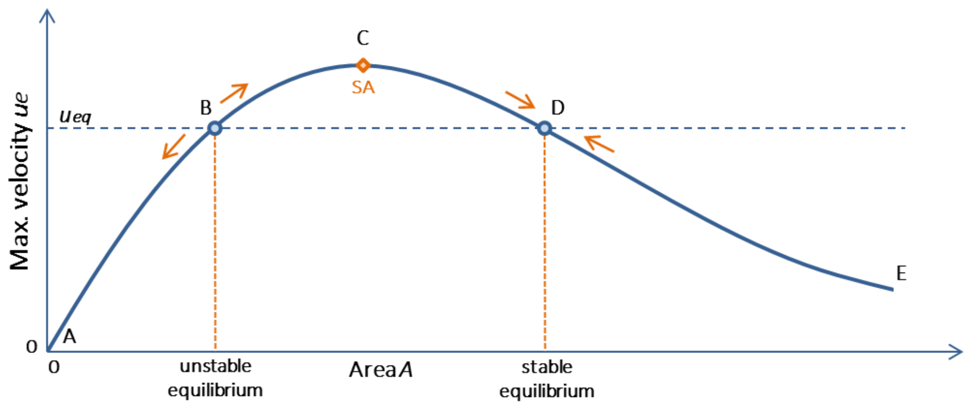

Figure 2.11 - Escoffier's curve, with indication of the inlet of the Santo André Lagoon (SA).

The velocity in the Santo André inlet is around 2 m/s two days after opening (Nahon et al., 2011). This suggests that the inlet of the Santo André Lagoon can be placed between B and D (e.g. around point C) on the curve and, according to theory, will move to the stable equilibrium (point D). This suggests the inlet cross-section will enlarge over time. In reality the inlet is not going to a stable equilibrium, but the inlet closes. This can be explained by the fact that the Escoffier curve is based on tidal processes (Van de Kreeke, 2004).

The maximum cross-sectional velocity is the maximum velocity during the tidal cycle and can be related to the tidal prism, which can be approximated by the following equation (Bosboom & Stive, 2012):

$$\hat{u}_e = \frac{\pi P}{A_e T} \tag{2.1}$$

Based on the measurements, the tidal prism (P), cross-sectional area (A) and tidal period (T) are calculated and defined for 11 March 2009. With values of $2.60 \cdot 10^6$ m^3 (P), 12.5 m^2 (A) and 12 hours (T), a velocity of 14.3 m/s is found. This velocity is extremely high. The reason for this high velocity probably may be the large tidal prism in relation to the cross-sectional area. This is also found in Pires et al. (2011). The tidal prism and cross-sectional area are not corresponding to the equilibrium curves of O'Brien (1969) and Jarrett (1976). The inlet of Santo André is very shallow and most the cross-sectional area of the inlet develops above MSL, therefore these theories are not applicable for this specific case.

Santo André is characterised by highly energetic wave conditions, which probably play a major role in the closure of the inlet (Nahon et al., 2011). Significant wave heights of about 2 meter occur along this coast, resulting in relatively large alongshore sediment transports that are probably important for the inlet's closure. In case of an open inlet, the short waves propagating perpendicular to the coast will enter the inlet and are breaking less, causing less undertow. But, on the other side, after breaching an ebb delta is formed. Perhaps this could cause early breaking of the short waves and long waves become relatively more dominant. Besides, strong currents occur in the inlet (large in- and outflows), which could affect the waves by current feedback on the wave field.

Summarising, the Santo André Lagoon with its inlet is a very complex system, in which short waves are expected to be relatively important due to the relatively steep beach profile of the adjacent coast. This includes processes as wave skewness, asymmetry and swash dynamics. Besides, long waves are expected to be important because of the cross-shore sediment transports that displace the ebb delta towards the coast. On top of that the tide plays a role in the morphological development of the inlet due to the strong in and outflows, enlarging the inlet channel. Different processes are influencing the morphological development. It is just a balance of these, which result in the inlet closure.

CHAPTER 3

Methodology

In this study, the morphodynamic model XBeach is used of which a short description is given in this chapter. This description is supported with a short explanation of the implementation of the important processes and parameters for this study (section 3.1). The description of the model set-up is given in section 3.2.

3.1 XBeach

The open-source program XBeach – eXtreme Beach behaviour model – is developed[4] to model the nearshore response to hurricane impacts. Processes as wave breaking, in surf and swash zone, dune erosion, overwashing and breaching are included in the model (Roelvink et al., 2009). XBeach is a 2DH (depth averaged) model that solves coupled short wave energy, flow and infragravity wave propagation, sediment transport and bed level change. An overview of XBeach is given in Appendix B.

The numerical model XBeach is used for this study to investigate the influence of physical processes involved in closure of the inlet in order to reproduce the closure. In previous research the morphodynamic model MORSYS2D was used (description in Appendix B). Reproducing the closure was not succeeded, because of not taken into account some processes (see Chapter 2.4). XBeach takes these processes (in particular the infragravity waves) into account; therefore this process-based model is used for this case in order to reproduce the inlet closure.

In the next section a short description is given of the implementation of the important processes in this study. For a more comprehensive description of XBeach one is referred to the XBeach manual (Roelvink et al., 2010) and several papers (e.g. Roelvink et al. (2009), McCall et al. (2010)).

[4] Developed by UNESCO-IHE, Deltares, Delft University of Technology and University of Miami, with funding and supporting of US Army Corps of Engineers (xbeach.org)

3.1.1 Model formulations

The important formulations, processes and parameters in this study are described in this section. A short description is given of the implementation of the waves in XBeach, together with the contribution of the roller and how the infragravity waves are solved. Another parameter described in this section is the wave-current interaction parameter (wci). Sediment transport can be influenced by the contribution of wave skewness and wave asymmetry, of which their implementation is also explained. The section ends with a short explanation of the implementation of the groundwater flow.

The short wave action balance is being solved on the scale of wave groups in XBeach. Wave input (H_{m0}, T_p, direction) is converted into a (2D) spectrum and from which random time series of waves are generated by XBeach. The wave action balance is given as follows:

$$\frac{\partial A}{\partial t}+\frac{\partial c_{g,x}}{\partial x}+\frac{\partial c_{g,y}A}{\partial y}+\frac{\partial c_{\theta}A}{\partial \theta}=-\frac{D_{waves}}{\sigma} \tag{3.1}$$

In which $A = E/\sigma$, E the wave energy and σ the intrinsic wave frequency is. The wave group velocity is represented by c_g (for x- and y-direction) and the velocity in directional space (c_θ) takes into account the refraction. The energy dissipation due to breaking waves is represented by D_{waves}. XBeach also includes a roller energy balance in order to redistribute energy from breaking waves to foam. Dissipation of short wave energy is used as a source term in the roller energy balance:

$$\frac{\partial E_{roller}}{\partial t}+\frac{\partial c_{g,x}E_{roller}}{\partial x}+\frac{\partial c_{g,y}E_{roller}}{\partial y}+\frac{\partial c_{\theta}E_{roller}}{\partial \theta}=-D_{roller}+D_{waves} \tag{3.2}$$

The infragravity waves are solved within the surface elevation, using the depth-integrated shallow water momentum and mass balance equations. Generalized Lagrangian Mean (GLM) formulations are used by XBeach to account for the wave-induced mass fluxes and the return flows. Where the Lagrangian velocity consists of the Eulerian and Stokes' velocity: $u^L = u^E + u^S$. The depth averaged GLM-shallow water equations are given in Equation 3.3 and 3.4 and result in the surface elevation (Equation 3.5):

$$\frac{\partial u^L}{\partial t}+u^L\frac{\partial u^L}{\partial x}+v^L\frac{\partial u^L}{\partial y}-fv^L-v_h\left(\frac{\partial^2 u^L}{\partial x^2}+\frac{\partial^2 u^L}{\partial y^2}\right)=\frac{\tau_{sx}}{\rho h}-\frac{\tau_{bx}^E}{\rho h}-g\frac{\partial \eta}{\partial x}+\frac{F_x}{\rho h} \tag{3.3}$$

$$\frac{\partial v^L}{\partial t}+u^L\frac{\partial v^L}{\partial x}+v^L\frac{\partial v^L}{\partial y}-fu^L-v_h\left(\frac{\partial^2 v^L}{\partial x^2}+\frac{\partial^2 v^L}{\partial y^2}\right)=\frac{\tau_{sy}}{\rho h}-\frac{\tau_{by}^E}{\rho h}-g\frac{\partial \eta}{\partial y}+\frac{F_y}{\rho h} \tag{3.4}$$

$$\frac{\partial \eta}{\partial t}=-\frac{\partial u^L h}{\partial x}-\frac{\partial v^L h}{\partial y} \tag{3.5}$$

Another parameter important in this study is the wave-current interaction ('wci'), which includes the feedback of currents on the wave propagation and the current refraction. In case of a shallow tidal inlet wave-current interactions play a major role in the dynamics of these systems. According to Dodet et al. (2013) the wave height at the mouth of the inlet is increased by the currents during ebb (up to 20%) and is decreased in the inlet (up to 40%). This occurs due to the current-induced refraction, steepness dissipation and partial blocking. During flood the increase and decrease of wave height is less, but still there. The wave height at the ebb shoal increased (up to 10%), due to current-induced refraction and is decreased in the inlet (up to 10%), due to the currents.

Turning the parameter 'wave current interaction' (wci) on, means that the Lagrangian velocities are taken into account in the wave action propagation speeds in x- and y-direction. Besides the current refraction terms in the propagation speed in θ-space are taken into account (Roelvink et al., 2010). The 'wci'-parameter is turned off by default. The sediment transports are calculated with a depth averaged advection diffusion equation, using the 'undertow' (u^E) (Equation 3.6), which is offshore directed in case of a closed system (u^S is onshore directed and u^L causes a zero net effect).

$$\frac{\partial hC}{\partial t}+\frac{\partial hCu^E}{\partial x}+\frac{\partial hCv^E}{\partial y}+\frac{\partial}{\partial x}\left[D_h h\frac{\partial C}{\partial x}\right]+\frac{\partial}{\partial y}\left[D_h h\frac{\partial C}{\partial y}\right]=\frac{hC_{eq}-hC}{T_s} \tag{3.6}$$

Onshore transports caused by wave asymmetry and skewness cannot be neglected, proven in previous research. Long wave asymmetry and skewness are solved within the surface elevation in the nonlinear shallow water equations in XBeach, but short wave asymmetry and skewness are not included. XBeach calculates only the amount of wave energy: $E = 1/8\rho gH^2$, it includes no information about the wave form. In order to take this into account the Ursell number (U_r) is used to express the wave asymmetry and skewness (Ruessink et al., 2009):

$$\begin{aligned}S_k &= \frac{0.79}{1+\exp\dfrac{-0.61-\log U_r}{-0.35}}\cos\left(-\frac{\pi}{2}+\frac{\pi}{2}\tanh\left(0.64/U_r^{0.60}\right)\right)\\ A_s &= \frac{0.79}{1+\exp\dfrac{-0.61-\log U_r}{-0.35}}\sin\left(-\frac{\pi}{2}+\frac{\pi}{2}\tanh\left(0.64/U_r^{0.60}\right)\right)\end{aligned} \tag{3.7}$$

To include the effect of wave skewness and asymmetry the Eulerian mean velocity is replaced by $u_{AV} = u^E + u_A$, where the velocity related to the wave skewness and wave asymmetry is given by:

$$u_A=\left(\gamma_{Sk}Sk-\gamma_{As}As\right)u_{rms} \tag{3.8}$$

Where γ_{Sk} and γ_{As} are the calibration factors, which can be changed in XBeach (between 0-1 and has a default value of 0.1). The short wave orbital velocity is represented by u_{rms}.

This gives a new advection-diffusion equation (Equation 3.9), with the new Eulerian velocity where the asymmetry and skewness are included. The velocity can become smaller or even positive, which causes less offshore sediment transport or even onshore directed.

$$\frac{\partial hC}{\partial t}+\frac{\partial hCu_{AV}}{\partial x}+\frac{\partial hCv_{AV}}{\partial y}+\frac{\partial}{\partial x}\left[D_h h\frac{\partial C}{\partial x}\right]+\frac{\partial}{\partial y}\left[D_h h\frac{\partial C}{\partial y}\right]=\frac{hC_{eq}-hC}{T_s} \tag{3.9}$$

For groundwater flow XBeach uses a simple model of Darcy (flow in laminar conditions):

$$u_{gw} = -k_x \frac{dp_{gw}}{dx}$$
$$v_{gw} = -k_y \frac{dp_{gw}}{dy} \tag{3.10}$$

In which the ground water flow is based on a relation between the groundwater head, the permeability (hydraulic conductivity in x- and y-direction) k and the horizontal velocity.

3.2 Model set-up

To reproduce the closure of the Santo Andre Lagoon, the simulation will be divided in several stages. These stages are shown in Figure 1.1. In this study the model starts at the second stage (B, March 11, 2009). As explained in Chapter 2.4, the velocities in the inlet peak 6 m/s (Pires et al., 2011). This is difficult to model and the main focus will be on the inlets closure, therefore this stage is not taken into account.

3.2.1 Grid

XBeach uses a rectilinear grid, but a curvilinear is also possible. In this study the rectilinear grid has a resolution of 40 x 80 m at the boundaries (in cross-shore and alongshore direction respectively), with a refinement in the transport zone and inlet of 2.5 m in cross-shore direction and 5.5 m in alongshore direction (Appendix Figure C.14). Smaller dimensions of the grid cells are preferable for the accuracy, but with increasing the amount of grid cells the calculation time will be increased as well. The calculation time of the first period (9 days), using the previous described grid, is more than three days. So a higher resolution is not acceptable due to a higher run time.

A curvilinear grid had also been made (to reduce the amount of grid cells and so the calculation time), but did not work for this case in XBeach (Appendix Figure C.15). This is probably due to the shape of the lagoon; there are too many dry cells at the dunes. It was possible to solve this, but time consuming and without expectations to be significant better than the rectilinear grid. The flow might be influenced by the strongly curved grid cells.

3.2.2 Bathymetry

The bathymetry is made of the available bathymetry samples. These data contain the measurements of the bathymetry, measured during low water. The measurements of the bathymetry offshore before opening are used for all the other moments; only the inlet and a small distance around it is measured for making the bathymetry of B, C, D and E. So for every bathymetry set, the bathymetry offshore is the same for every moment, only the inlet is varying.

Measurements do not have the same resolution everywhere. The distance between the measuring points are varying between 10-20 m in the inlet and have a larger distance in front of the inlet and lagoon. For example, comparing the samples of B to C, D and E, less data points for the flood delta are measured. Besides, in these samples (see Appendix C.3, Figure C.4 – C.11) a gap between the ebb delta and further offshore is visible. Therefore the accuracy of the samples is doubtable.

The bathymetry and model domain used for this study is shown in Figure 3.1. The measured bathymetry is linear extended from a depth of -15 m (limit of the measured bathymetry) to a depth of -25 m.

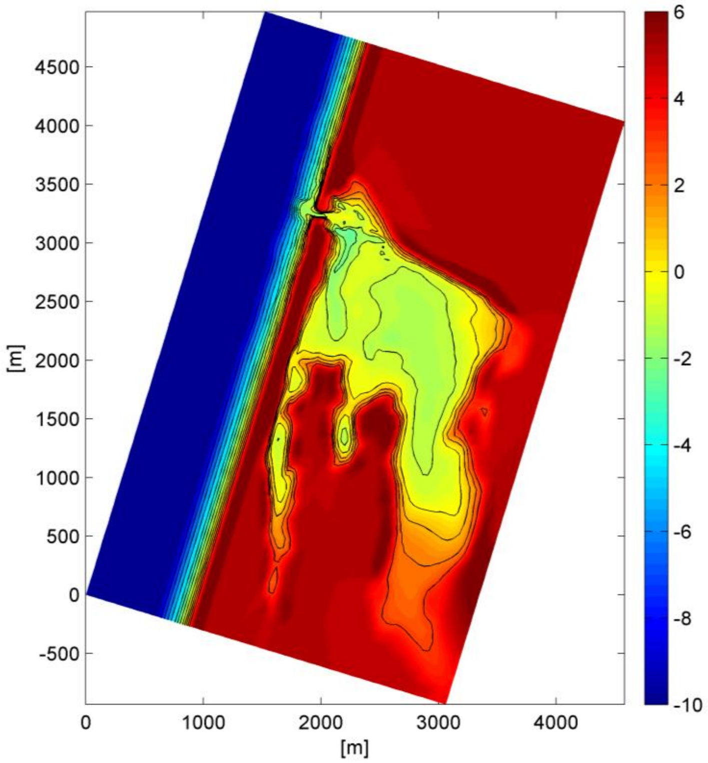

Figure 3.1 - Bathymetry of model domain [m] MSL, with the origin (-60436, -175910) in 'DATUM73' coordinates (which is 38°4'48N 8°49'12W)

3.2.3 Boundary conditions

Tidal and wave data are obtained from buoy data. For the water levels a tide gauge in the harbour of Sines is used and a directional buoy moored in deep water (70 m) offshore Sines is used for the wave data. These measured data show several large gaps (see Appendix C.1 and C.2) and thus the data is not sufficient to use for this study. Therefore the tidal and wave forcing is obtained from regional tide and wave models (Bertin et al. (2012) and Guillaume Dodet et al. (2010)).

Tide

For tidal forcing, the XBeach model is nested in the regional tide and surge model of Bertin et al. (2012). This regional tide and surge model has a RMSE of <0.05 m for the surface elevation. A comparison of the measured data and the data from the model can be found in Appendix C.1.

The resolution of the used grid in the model of Bertin et al. (2012) is about 2-3 km along the coast, where the water levels in the region are not varying a lot, it is not necessary to use time series of water levels for several points for this study.

Wave

For the wave forcing the wave data is obtained from the North-East Atlantic Ocean wave model of Dodet et al. (2010), which is also nested in the XBeach model. This spectral wave model has a level of accuracy that enables reproducing Hs and Tp with errors of the order of 10% (Guillaume Dodet et al., 2010). The comparison of the measured data and the data from the model can be found in Appendix C.2.

3.2.4 Settings

Some settings are changed instead of using default, before calibrated. An overview of these is shown in Figure 3.2.

```
PARAMS.TXT

D50           = 0.001150
D90           = 0.001180

eps           = 0.050000
avalanching   = 1
nrugdepth     = 1
tidelen       = 4195
depfile       = bed.dep
posdwn        = -1
nx            = 155
ny            = 125
alfa          = 343

vardx         = 1
xfile         = x.grd
yfile         = y.grd
xori          = 0
yori          = 0

thetamin      = -60
thetamax      = 60
dtheta        = 15
```

```
tstop         = 777600
CFL           = 0.700000
morstart      = 100

depthscale    = 1
swave         = 1
lwave         = 1
sedtrans      = 1
morphology    = 1
smax          = 1

zs0file       = tide.txt
tideloc       = 1
instat        = jons
bcfile        = filelist.txt

outputformat  = netcdf
rugdepth      = 0.100000
tintm         = 3600
tintp         = 60
tintg         = 1800
tstart        = 0
```

Figure 3.2 - Params.txt, input parameters before calibration

The sediment in the Santo André Lagoon is coarse, with a D50 of 1.15 mm and D90 of 1.18 mm. In literature it is found that the orientation of the adjacent coast is N15°E, but in the model a better fit between the bathymetry and grid is with an orientation of N17°E. Therefore alfa has a value of 343°. The waves and tide are entering the model reasonable in the beginning, without any wiggles. Therefore the morphology starts already after 100 s (morstart). CFL, the courant number, is stated at its default value of 0.7. A value of 0.9 has also been used, which resulted in shorter calculation time, but in a less stable model. XBeach is more stable with a value for CFL of 0.7 and therefore this value is used. Smax is an engineering tool in XBeach and has yet not been tested very well. The parameter is used as the maximum Shields parameter. In this study it is stated at 1 to reduce the increasing depth in the inlet channel.

CHAPTER 4

Calibration

Every coastal system is different, so every modelling case is different and different values for parameters need to be used. Default settings are not always enough in order to get reasonable results from modelling. Therefore some calibration needs to be done. Based on (measured) data, some parameters are adjusted in order to get comparable results (e.g. for water levels or sediment transports).

Calibration for this study is done in two parts. In the first calibration part, the tide is calibrated (section 4.1). Measured data of the water levels off shore and in the lagoon are used for this. In order to obtain corresponding water levels the bottomfriction is adjusted. For the second calibration part (wave) parameters are used to calibrate the sediment transport (section 4.2). This is based on qualitative rather than measured data.

4.1 Calibration of hydrodynamics

During the artificial opening of the inlet in 2009, water levels in the lagoon were measured with a pressure transducer and water levels outside the lagoon were obtained from the tide gauge in the harbour of Sines. The measurements of the lagoonal water level were recorded every 10 minutes, starting shortly before opening until two days after the inlet closure (Pires et al., 2011) and for the ocean tide every 6 minutes the water level was recorded. The location of the measurements in the lagoon is shown in Figure 4.1. Both time series are shown in Figure 4.2.

The point in the lagoon is at a depth of around -1m, but the recorded water level is never below 0.3 m. Regarding the vertical reference of the point, two comments can be made:

1) The vertical position was not determined accurately, because the sensor was moored and a DGPS could hardly be used to measure its position under the sea surface. Therefore empirical tuning cannot be avoided comparing with the data.
2) The water level in such lagoons is always a little above oceanic MSL, therefore a point in the lagoon located a little below the oceanic MSL will hardly dry.

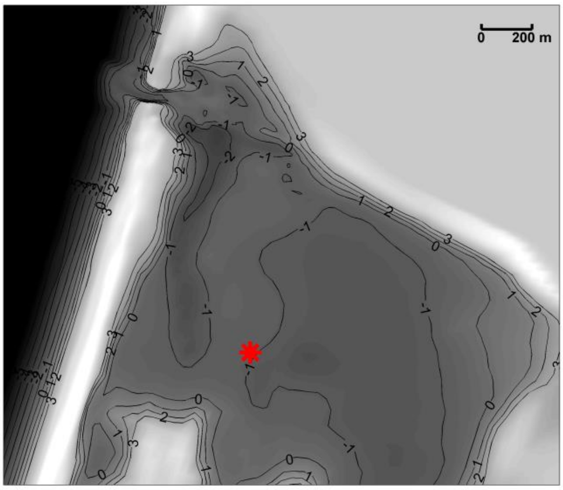

Figure 4.1 - Location of measured water level inside the lagoon.

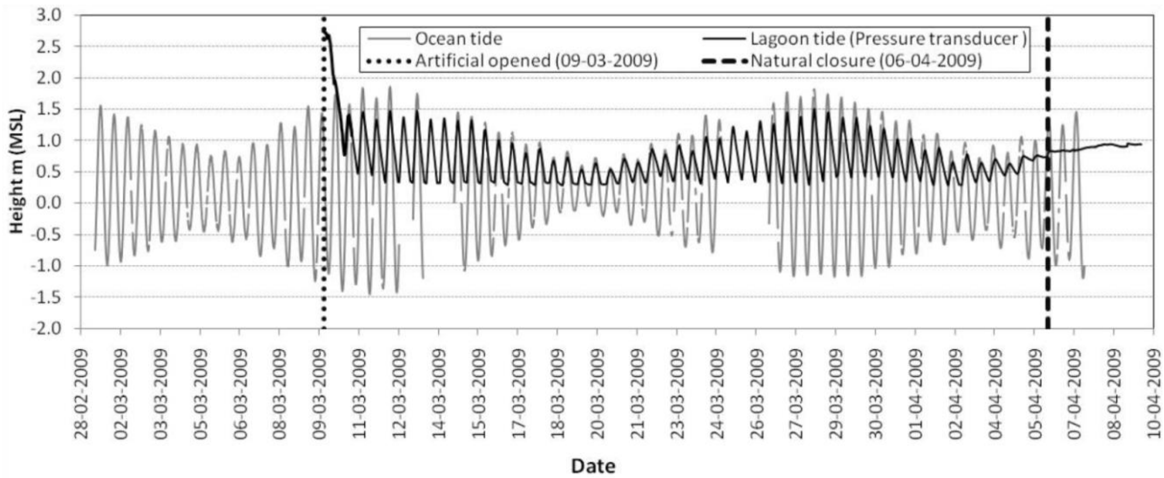

Figure 4.2 - Time series of water level variation in the ocean and lagoon (Pires et al, 2011)

The recorded lagoonal water level data is used for calibration. Besides the water level off shore and the water level in the lagoon, the tidal range between both water levels is also shown in Figure 4.3. In the upper plot in the figure, the oceanic water level is shown (data in blue and model in orange). The middle plot shows the lagoonal water level and the bottom plot shows the tidal range ratio of both the oceanic and lagoonal water level.

Simulations are carried out with default settings and some adjusted ones (Appendix D). These simulations did not result in corresponding water levels. The range of the water level in the lagoon is too large compared to the tidal range ratio of the measured water level (Appendix Figure D.1). In order to reduce this range ratio and resulting in a corresponding water level, the bottomfriction coefficient is adjusted. The default Chézy value in XBeach is 55 $m^{0.5}/s$, which resulted in an underestimation of the bottomfriction. The higher bottomfriction is to be expected and can be explained by the relative coarse sediment (d50=1.15mm) and the presence of large bed forms as well as hydraulic jumps, as explained in Nahon et al. (2011).

After a few optimisation steps (varying the values between 40 and 20 $m^{0.5}/s$), an optimal Chézy value of 35 $m^{0.5}/s$ is found. The corresponding water level with a Chézy value of 35 $m^{0.5}/s$

compared with the measured data is shown in Figure 4.3. The results of the varying Chézy values are shown in Appendix Figure D.2.

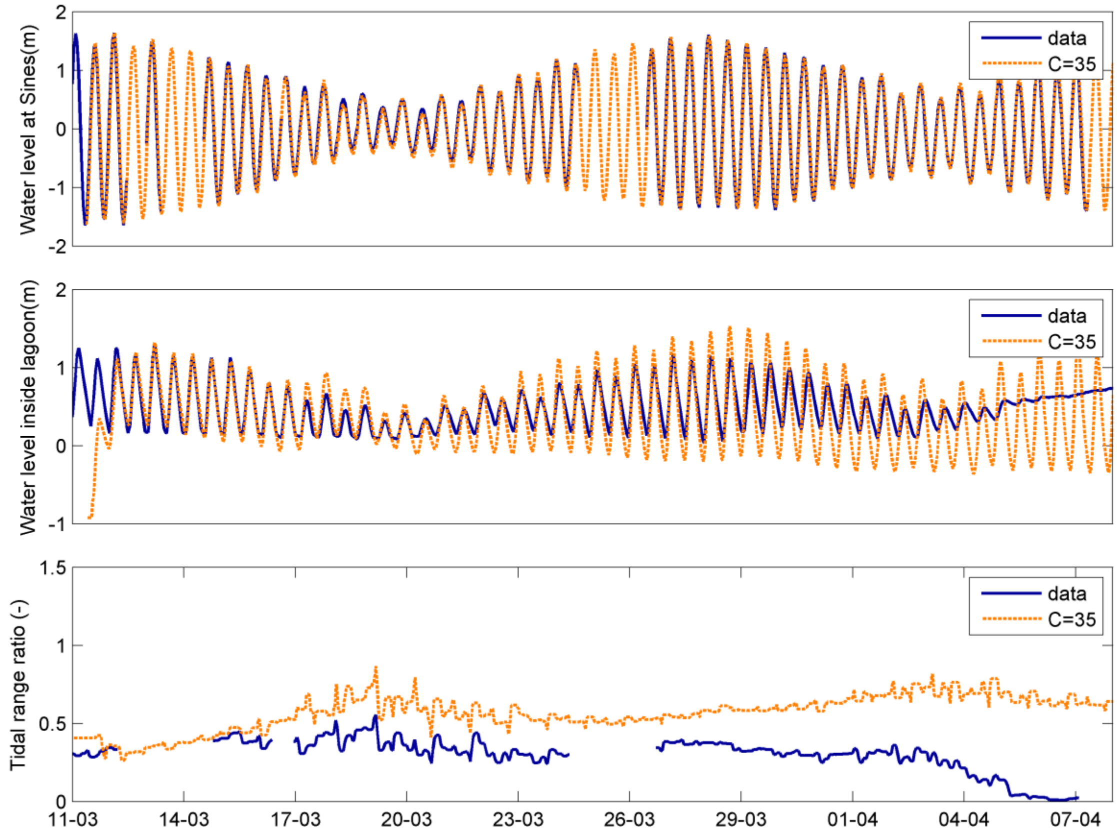

Figure 4.3 - Calibrated water level compared to measured water level, with Chézy value of 35 $m^{0.5}/s$.

As can be seen in Figure 4.3 until March 16th the water levels are corresponding quite well. In order to quantify this correspondence, the Root Mean Square Error (RMSE) can be calculated:

$$RMSE = \sqrt{\frac{\sum_{t=1}^{n}(zs_{t,data} - zs_t)^2}{n}} \tag{4.1}$$

For the period until March 16th, an error of about 1.02 cm is found for the lagoonal water level. Including the remaining period an error of 60.43 cm is found for the lagoonal water level, which is too large. The reason for this large error may be the result of the changing bathymetry, in particular the increasing inlet dimensions of width and depth. An increasing depth better tidal propagation and less damping and therefore the water levels are changing easier.

In Table 4.1 an overview of the RMSE for the different Chézy values is given. Comparing the given values from the first column, the RMSE is the smallest in case of C = 35. After four days this RMSE is even smaller, but increases after this period. In Figure 4.3 the water levels correspond less after March 17th. According to these RMSEs it can be concluded that a bottomfriction with a Chézy value of 35 $m^{0.5}/s$ is suitable.

RMSE [m]	*2.75 days*	*4 days*	*6 days*	*8 days*
C = 55	2.144	3.5544	3.5521	3.34
C = 40	0.4269			
C = 35	0.1011	0.0102	0.2406	0.64
C = 30	0.1402			
C = 20	0.3597			

Table 4.1 - RMSE for several Chézy values

4.2 Calibration of sediment transport

After calibration of the hydrodynamics, the results show erosion at the shoreline and sedimentation in the surf zone that leads to a milder beach slope (Figure 4.4). XBeach tends to erode the shoreline, leading to a milder slope. It is known that XBeach is not performing very well near the waterline which often results in an eroding shoreline. For shorter time scales (~1 day) in combination with high energy conditions (which is the most common XBeach application) this is usually no serious problem, because there is a large net offshore transport which is much larger than this 'eroding shoreline' effect. When looking at milder conditions, the effect becomes relatively more important, and when increasing the simulation time the model will keep eroding the shoreline leading to a milder beach slope.

The eroding shoreline is not realistic, because such tremendously erosion was not observed in reality. There is no data available to compare the beach profile. The only available 'data' for this is anecdotal; the knowledge of a more or less stable beach profile during the period of the open inlet. With this knowledge further calibration is done by calibrating (wave related) parameters. Changing these parameters will influence the sediment transport and so the beach profile.

Wave related processes, such as wave asymmetry, wave skewness and the roller are adjusted in order influence the sediment transport and result in less erosion (in this case). Other parameters, such as wetslope, groundwater flow contribution and hmin are also adjusted in order to stabilize the beach profile. This calibration is described in the next sections.

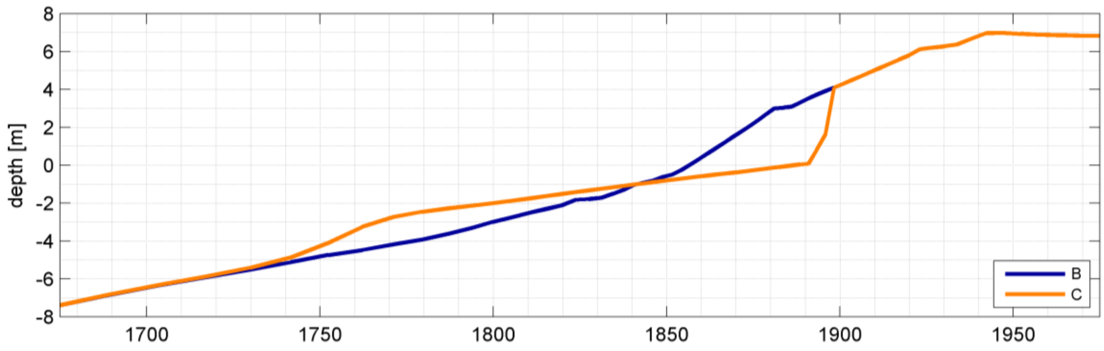

Figure 4.4 - Cross-section of the beach profile north of the inlet. Blue line indicates the initial beach profile (B) and the green line indicates the beach profile after 9 days (C).

4.2.1 Wave asymmetry and skewness

The coast is eroding and the beach profile is flattening in Figure 4.4. As explained in section 2.2.2 wave asymmetry and wave skewness can influence sediment transport and may be important for beach profile development. In Chapter 3 the implementation of these parameters in XBeach is described. Both processes are parameterised and adjusted with factors in XBeach. These factors (both asymmetry and skewness have an independent factor) can be adjusted in order to get the right result related to wave asymmetry and wave skewness. Results of this calibration part can be seen in Appendix Figure D.4 – Figure D.7.

The wave asymmetry and skewness factors have a default value of 0.1 and can be varied between 0 and 1. The maximum and minimum values (0 and 1) are used to see the impact of these factors. Using both the maximum value of wave asymmetry factor and skewness factor, this resulted in enormous accretion. Although there is more accretion, the gradient of the beach slope is still changing unrealistic according to the observations (Appendix Figure D.4).

The minimum and maximum values were not resulting in satisfying results, therefore several simulations were performed, varying the wave asymmetry coefficient between 0-0.6 with steps of 0.05 and for the wave skewness the range used is between 0-0.3, with steps of 0.1. The results of these simulations are shown in Appendix Figure D.3 – Figure D.7.

For values between 0.4-0.6 for the wave asymmetry factor, resulted in a comparable beach slope in the transport zone, but the shoreline moves offshore with ~20 m. The wave skewness coefficient has also been adjusted, but seems to have less influence on the changing beach profile than the influence of the wave asymmetry. Turning the wave skewness coefficient off, the results are better, but it means that waves are not skewed at all. As explained in section 2.2.2, waves show some skewness when propagating towards the shore, because the waves are feeling the bottom. There is no data about the skewness of the waves, but assuming there is always some skewness, the default value of 0.1 is used.

4.2.2 Wetslope

'Wetslope' is the parameter for the critical bed slope under water. When the slope is exceeding a certain value, avalanching occurs. The default value for 'wetslp' has been set to 0.3, which corresponds to a beachslope of 3:10. The beach of the adjacent coast along the Santo André inlet has a slope of 1:10. Therefore the value for this calibration parameter is set to 0.1.

4.2.3 Groundwater flow

The sediment at the Santo André Lagoon is quite coarse, with a d50 of 1.15 mm. This is larger than the default settings for the sediment. Therefore the permeability of the beach is to be expected different than using the default values for the sediment. For a larger sediment grain, higher permeability is expected. Permeability has influence on the ground water flow as well as on the stability and thus erosion and accretion of the beach profile.

When a wave is running up the beach, the water will infiltrate into the beach. Infiltration during the uprush and exfiltration during the backwash of the wave causes groundwater flow in the beach. This groundwater flow can be important for the sediment transport. The infiltration has a stabilising effect on the beach slope, because of downward directed flow gradients. During backwash, the exfiltration causes the opposite effect. Depending on the duration this will promote a net onshore or offshore directed sediment transport. In this case the beach slope is relative steep and it has larger grain sizes. Increasing the permeability is expected to have a positive effect on the beach slope; less erosion.

In XBeach the groundwater flow is implemented with a simple model of Darcy (flow in laminar conditions):

$$u_{gw} = -k_x \frac{dp_{gw}}{dx} \tag{4.2}$$

In which the ground water flow is based on a relation between the groundwater head $\frac{dp_{gw}}{dx}$, the permeability (hydraulic conductivity in x-direction) k_x and the horizontal velocity u_{gw}.

The permeability can be defined using different expressions (e.g. Hazen (1911); Carman (1937); Kozeny (1927); Krumbein and Monk (1942) and Hegge (1994).) Because limited data is available, the (relatively simple) expression of Hazen (1911) can be used to make an estimation of the permeability:

$$k = C \cdot D_{10}^2 \tag{4.3}$$

Where C is an empirical constant (value between 0.01 and 0.015) and D_{10} the 10% sediment diameter.

But the equation of Hazen is less sophisticated and it is also not known how well this equation predicts the permeability of the beach sediment (Masselink & Li, 2001). Therefore the equation of Hegge (1994) is used to estimate and calculate the hydraulic conductivity. Hegge (1994) found an equation based on in situ measurements of permeability on a number of beaches:

$$k = 0.0062 \cdot D_{50}^2 \tag{4.4}$$

Based on this equation the hydraulic conductivity should be around 0.008 m/s with this size of sediment.

In XBeach a default value of 0.0001 m/s is used and belongs to finer sediment. The value of 0.01 m/s is the maximum used in XBeach. Several simulations are performed, with values of 0.0001, 0.001 and 0.01 m/s, resulting in least erosion in the case of a hydraulic conductivity of 0.01 m/s. Although the conductivity according Hegge is slightly lower with this sediment, a value of 0.01 m/s is used. Calculating the conductivity with the equation of Hegge is only depending on the sediment size. Results with a value of 0.01 m/s show slightly better results and therefore this value is used.

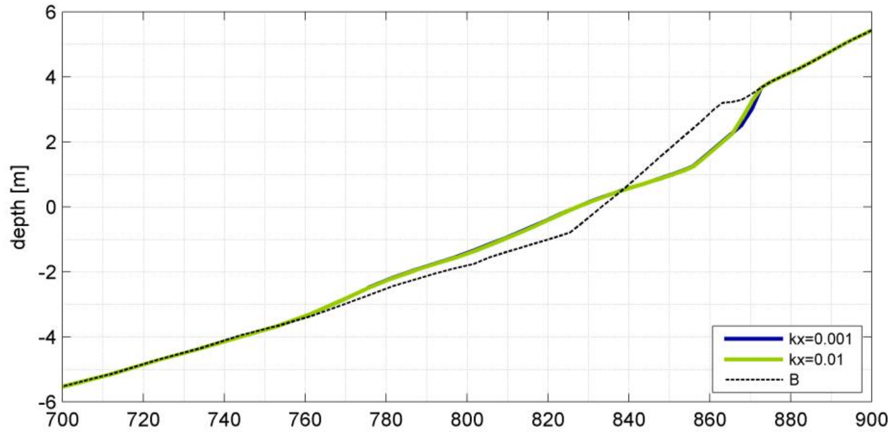

Figure 4.5 - Beach profile after 3 days, with asymmetry factor of 0.25 and skewness factor of 0.1

4.2.4 Roller

Another coefficient, to influence the sediment transport, is the roller contribution. As explained in Chapter 3.1 a roller energy balance is included in XBeach in order to redistribute energy from breaking waves to foam. In this case the waves are approaching the coast and are breaking (i.e. this is corresponding with the collision regime of Sallenger (2000)). The waves and rollers carry the mass flux and returns offshore as a return flow or a rip-current. Erosion occurs by these offshore directed flows and keep the erosion process on going by removing sand from the slumping dune face (Roelvink et al., 2009).

This roller coefficient can be turned on or off in XBeach. Turning off this ‘button’, the contribution of the roller (in the Stokes’ velocity and in the radiation stress) will be turned off. By turning off this contribution the offshore transport is reduced and less erosion occurs. This results in a better corresponding beach profile.

Because the contribution in the radiation stress is also turned off, the influences of the long waves might be affected as well. In order to verify this, a simulation is done with the roller contribution of the Stokes’ velocity turned off and the contribution of the radiation stress turned on. The effects on the waves are shown in Figure 4.6.

The waves are comparable for all the three simulations during the first day. After this period the waves are slightly different, a result of the changing beach slope (see Figure 4.7). During the first day, this is not changing that much.

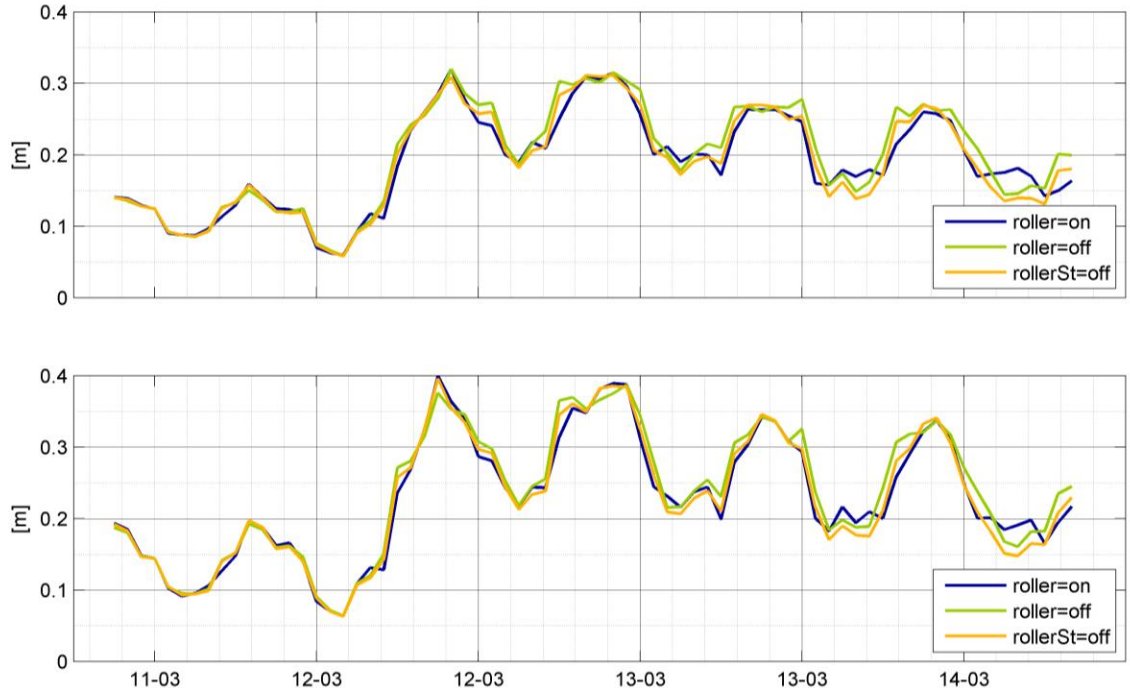

Figure 4.6 – Waves (at depth of -4.5m, upper; at depth of -2m, bottom) from simulations where roller is turned on (blue), where roller is turned off (green) and where contribution of Stokes' velocity is turned off (orange).

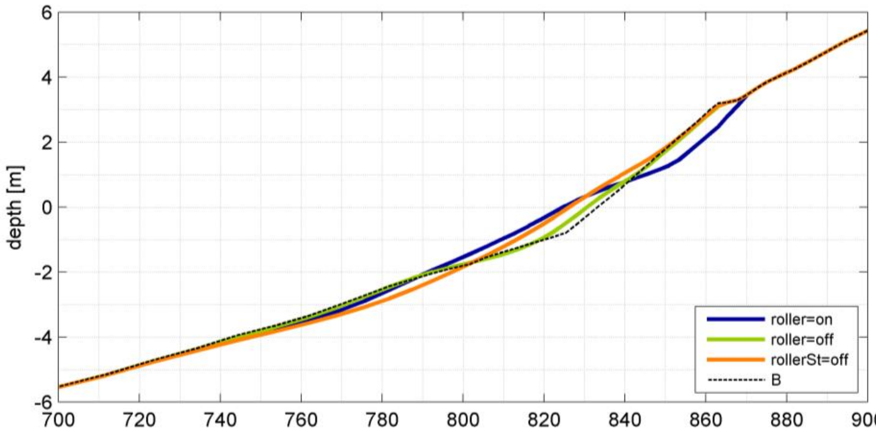

Figure 4.7 - Beach profile after 3 days (starting with B), belonging to waves of Figure 4.6

4.2.5 Hmin

Although hmin is not really verified with the model, the value of the parameter is adjusted from 0.2 m (default value) to the maximum value (in XBeach) of 1 m. As explained in chapter 4 'hmin' reduces the return flow and correspond to the threshold water depth above which the Stokes' drift is included. To reduce this return flow and thus the erosion, the value of the parameter needs to be increased. With this change the beach profile is almost 'perfect'; is it almost the same as the initial beach profile as can be seen in Figure 4.8.

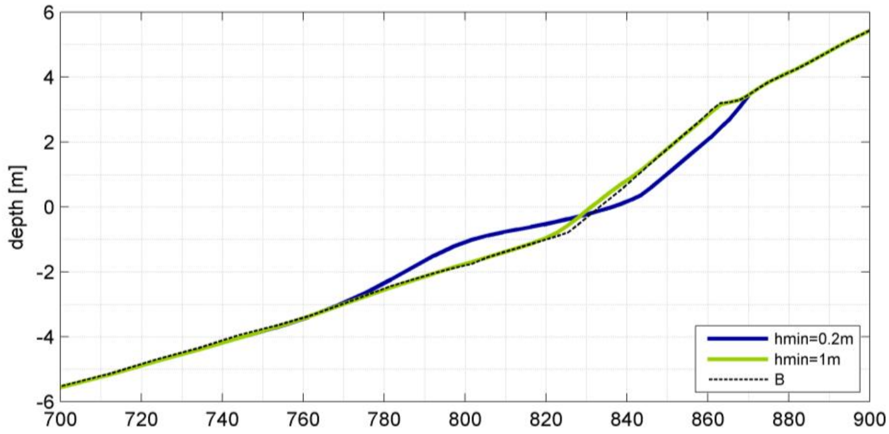

Figure 4.8 - Beach profile with hmin=0.2 m (blue and yellow line) and hmin=1 m (green and red line), after 9 days

4.3 Conclusion

Only quantitative data for water level is available to calibrate the model. Further calibration with measured data is therefore not possible. There is anecdotal knowledge of the more or less stable beach profile. Using this, calibration is performed with wave related parameters and some other parameters are adjusted to create a more or less stable beach profile.

Several parameters are adjusted in order to reduce the erosion (as can be seen in Table 4.2); wave asymmetry and wave skewness factors, groundwater flow, roller contribution and the hmin and wetslp.

	XBeach	*Default*	*Min.*	*Max.*	*Range*	*Used value*
Wave asymmetry	*facAs*	0.1	0	1	0-0.6,1	0.25
Wave skewness	*facSk*	0.1	0	1	0-0.3, 1	0.1
Hydraulic conductivity	*kx*	0.0001	0.00001	0.01	0.0001,0.001,0.01	0.01
Roller	*roller*	1 (=on)	0 (=off)	1	On/off	Off
Stokes' drift depth	*hmin*	0.2	0.001	1	0.2, 1	1
Wetslope	*wetslp*	0.3	0.1	1	0.1	0.1

Table 4.2 - Overview calibrated and adjusted parameters and its values

These settings found after calibration are used to model the development of the inlet in order to understand the evolution and reproduce its closure. An overview of the input can be found in Appendix D.3. Results of these simulations are shown and explained in Chapter 5.

CHAPTER 5

Results

The results of the simulations with XBeach are shown in this chapter. Comparison of the results with a uniform bottomfriction coefficient and with a spatial bottomfriction coefficient are shown and explained. General explanation of the morphological development in the model is given thereafter. This chapter ends with the results of the influence and the contribution of the physical processes; long waves and current feedback on the wave propagation ('wci').

5.1 Uniform bottomfriction

Simulations with the settings found after calibration are performed. Starting from stage B a simulation is performed of which the results are shown in Figure 5.1. In the upper row, the bathymetry of the measured data is shown and in the bottom row, the model results are shown. Both series are from B till E (two days after opening until 3 days before closure).

In the period from B to C a spit is formed. Comparing both bathymetries for stage C, large difference in spit forming can be observed. The model results show a small spit, which is below MSL, while in the measured bathymetry the spit is situated above MSL. The shape and location of the spit is more or less comparable. The modelled spit is slightly more offshore directed. In the same stage the ebb delta is vanished in the measured data, but in the model results, the contour lines of the ebb delta are still visible. South of the inlet in the model results a sand bump can be seen, which is not noticeable in the measured bathymetry. The inlet channel is increasing in depth and width, which is comparable to the measured data. Figure 5.2 shows the cross section of the inlet (measured and modelled) for every stage, in which the comparable depth and width can be seen.

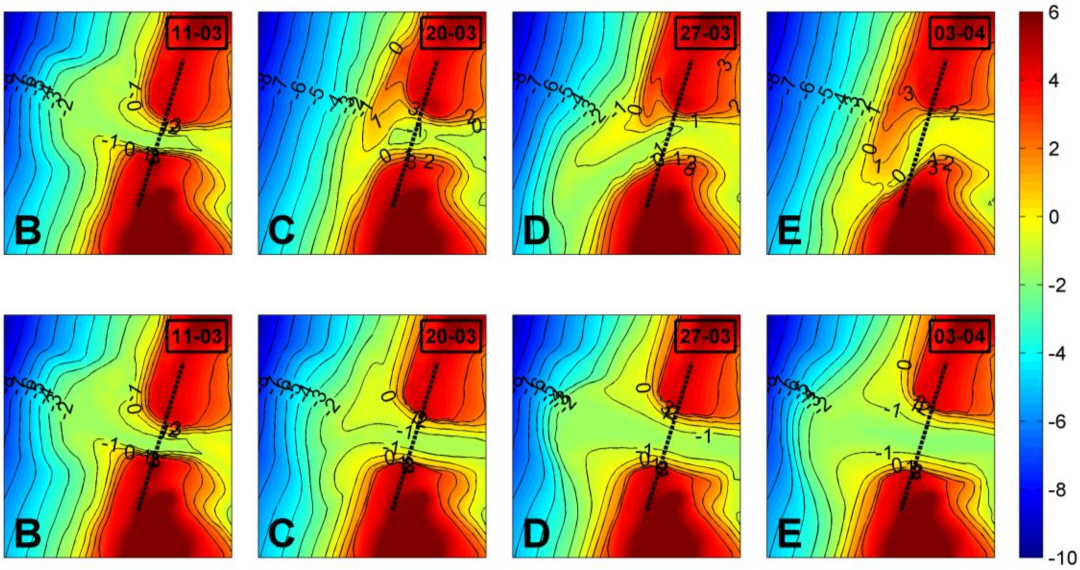

Figure 5.1 – Bathymetry inlet [m] MSL; measured (up) and modelled (bottom), with location of cross-section inlet.

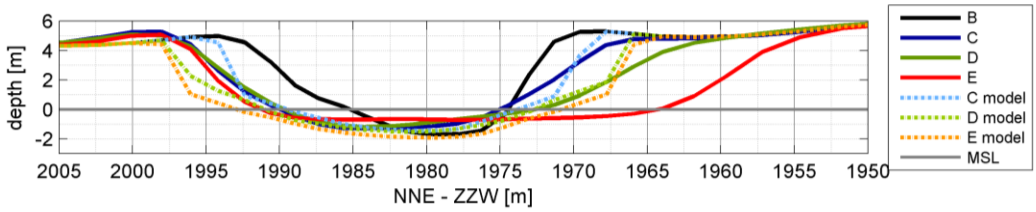

Figure 5.2 - Comparing cross-section of the inlet; measured vs. modelled

The small spit formed in stage C is completely disappearing in the second period of the model results (C to D). The ebb delta is visible and is quite comparable with the bathymetry of stage B. Only the inlet has increased in width and depth in D (comparing to B). Comparing this bathymetry to the measured bathymetry, it is not corresponding. The spit is still visible in the measured bathymetry and is pointed offshore, developing an inlet channel directed southward. The modelled cross-section of the inlet is quite comparable with the measured cross-section; only the channel becomes shallower in the measured data, while in the model the channel is increasing in depth. The difference in depth is more than a meter (difference between the red and orange-dotted line in Figure 5.2). Another difference between these cross-sections is the width. The measured cross-section is enlarging, which is a result of the meandering channel directing more southward. This is not the case in the model and therefore the width is not increasing.

It seems that tide plays a dominant role in the development of the inlet in the model, because the inlet is enlarged without forming a spit. There may be an underestimation of the longshore transport (LST), due to the fact the spit is not formed properly. Besides the cross-shore movements and cross-shore transport (CST) may be underestimated as well, regarding the ebb delta that is not disappearing.

According to these hypotheses some wave breaking parameters were adjusted to increase onshore movements, but did not cause a disappearing ebb delta in stage C.

The calibrated bottomfriction is relatively large, it may be too large for the adjacent beach, but sufficient for corresponding water levels. When it is too large for the adjacent coast, the LST may be underestimated. For the adjacent coast the default value (55 $m^{0.5}/s$) of the bottomfriction coefficient should be sufficient. Therefore in space varying bottomfriction is used with a Chézy value of 55 $m^{0.5}/s$ offshore and a value of 35 $m^{0.5}/s$ in the inlet and the lagoon. To ensure a smooth transition a linear transition zone of several grid cells is included.

Another method for the bottomfriction can be used in XBeach as well: White-Colebrook, in which the bottomfriction (C) is calculated depending on the depth (h), using the grain diameter ($D90$). It is used in XBeach as follows:

$$C = 18 * \log\left(\frac{4h}{\mathrm{D90}}\right) \tag{5.1}$$

While it seems to be a useful method to calculate the bottomfriction (i.e. the bottom is changing, therefore the depth is changing, and thus the bottomfriction need to change as well), the bottomfriction coefficient values give too large values converting to Chézy values in the model (e.g. underestimation of the bottomfriction).

5.2 Spatial varying bottomfriction

Simulations with spatial varying bottomfriction are used to investigate the behaviour of the inlet and the processes involved in the inlet closure. Starting from stage B a simulation is performed of which the results are shown in Figure 5.3. In the upper row, the bathymetry of the measured data is shown and in the bottom row, the model results with a spatial varying bottomfriction are shown. Both series are from B till E (two days after opening until 3 days before closure). In Figure 5.4 the cross-sections of the inlet, both measured and modelled, are shown for every stage.

As can be seen in Figure 5.3 the model results show some comparisons with the measured bathymetry, but also several differences. In the first period (B to C) a spit is formed, but in the model results this spit is below MSL, while it is above MSL in the measured bathymetry. Besides, the ebb delta has not disappeared in the model results as it is in the measured results. In the next period the spit has disappeared and an ebb channel has formed as well as an ebb delta. It seems the tide has larger influence on the system as it is spring tide during stage D, because of the disappearing spit and forming ebb delta in the model. In the last stage a small spit is formed, but again below MSL and not above MSL as can be seen in the measured bathymetry. Still the contours of the ebb delta are visible. During the whole period (B to E) the inlet dimensions are comparable (Figure 5.4), except the inlet is increasing in depth in the model and in the last stage not widening. The latter is the result of the channel that is not moving in southward direction in the model.

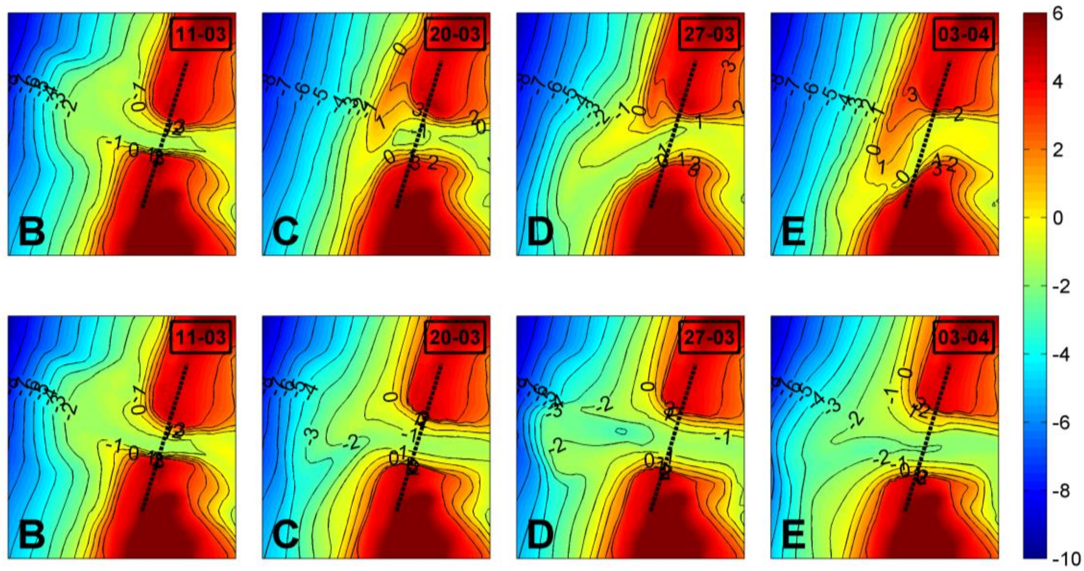

Figure 5.3 - Bathymetry inlet [m] MSL; measured (up) and modelled (bottom), with location of cross-section inlet.

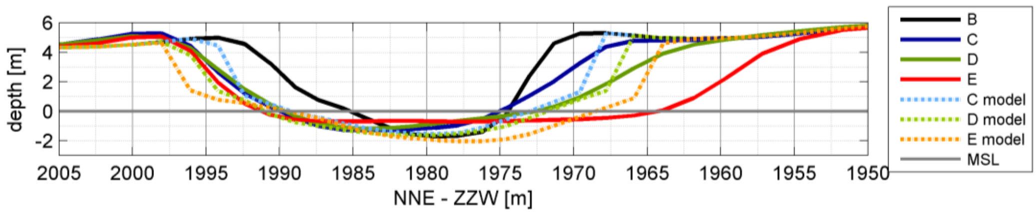

Figure 5.4 - Comparing cross-section of the inlet; measured vs. modelled

Because there is a spit formed in the model, but smaller than in the measured data and the ebb delta is not disappearing, it seems onshore transports are underestimated or offshore transports are overestimated. Therefore the inlet velocities are calculated and are presented in Table 5.1. The velocities are extremely large during the total period, as can be seen in Figure 5.5. Especially at the mouth of the inlet (indicated as 'west' in Figure 5.5), the velocities are high and offshore directed (negative), causing a strong outflow of water.

Velocity inlet	*Max. ebb [m/s]*	*Max. flood [m/s]*
west	4.04	2.16
east	1.37	2.68
middle	2.92	3.03

Table 5.1 - Maximum ebb and flood velocities in the inlet

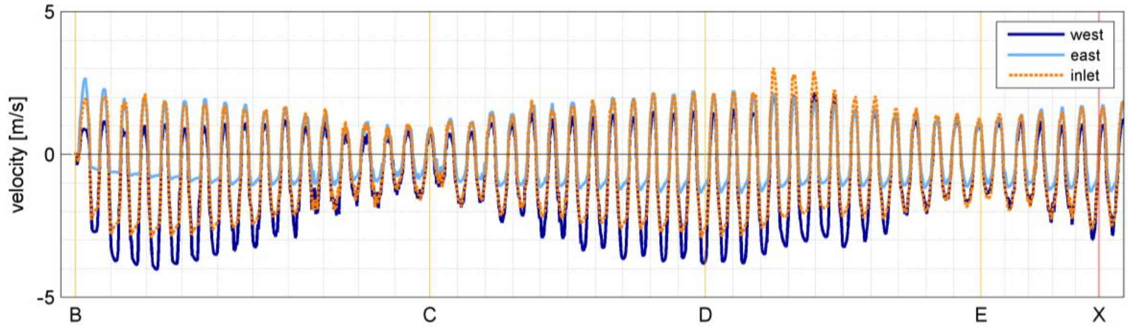

Figure 5.5 - Velocities in the mouth of the inlet (west), middle of the inlet (inlet) and east of the inlet (east). Locations of the measurements are the same as indicated in Figure 5.6 in the bottom plot. (Negative is associated with ebb currents and positive with flood currents.)

The volumes from the model results are compared with the measured volumes for the first period (B to C), as described in Chapter 2.5. It is difficult to compare the volumes equally, especially for the ebb delta and spit, because the spit is not above MSL in the model as it is in the measured bathymetry. But the total volume change of the first area (ebb/spit area) is comparable, which suggests the ebb delta need to be moved more onshore in the model. In Table 5.2 the volume changes are shown, in which the bold volumes are comparable.

The volumes for the first period (B to C) in the inlet channel are comparable, but are not for the lagoon. The measured volume change is larger than the modelled volume change. More sediment should have been pushed into the lagoon, forming a flood delta according to the measured data. But this is uncertain, because the measurements of stage B are less in number than the measurements of stage C and may be less accurate for the flood delta (Appendix Figure C.8 and Figure C.9).

Volume [$*10^5$ m^3]	*Measured*	*Model*
Offshore (<-7.5m)	-0.257	-0.022
Ebb delta (-7.5 - -0.5m)	-1.100	-0.316
Spit (-0.5m)	0.603	-0.037
Dunes (> 3m)	**-0.012**	**-0.018**
Inlet channel (<-0.5 m)	**-0.105**	**-0.370**
Inlet dunes (>-0.5 m)	**-1.549**	**-1.501**
Total ebb/spit	**-0.766**	**-0.392**
Total inlet	**-1.643**	**-1.871**
Total flood delta/lagoon	2.122	0.249
Total system	-0.287	-2.013

Table 5.2 - Volume changes from stage B to C; measured vs. modelled

In Figure 5.6 the cumulative longshore transport (LST) and cross-shore transport (CST) are shown to visualise to where the net transport is directed. The plots left of the transport plots show the location where the transports are calculated. The LST north and south of the inlet is comparable (until stage D) and has a net transport southward directed. Shortly after stage D the LST increases significantly and a large difference between the transport north and south of the inlet is visible. At the same moment large waves are acting on the coast, as can be seen in Figure 5.8 in the upper plot. The wave height almost increases up to 3 m and are directed from 310°-330° (which corresponds to a wave angle of incidence of 45°-60°). This results in large sediment transports as explained in chapter 2.3. During the period of these relatively high waves spring tide occurs (bottom plot Figure 5.8) and causes large in and outflows in the inlet, resulting in a spit formation in only three days (Figure 5.7). There is not a significant change in the CST, which is still dominant offshore, as shown in the bottom plot of Figure 5.6. But the measurements of these transports are in the inlet and not in front of the inlet. Therefore the sediment 'pushed' onshore causing spit formation is not visible in the CST. The green line corresponds to the eastern inlet cross-section and shows a transport directed into the lagoon. The orange line corresponds to the cross-section at the mouth of the inlet and shows a larger offshore directed sediment transport. This net offshore directed sediment transport of the inlet is visualised by the blue line that corresponds to the cross-section in the middle of the inlet. So, the CST seems to be dominated by the tide; following the same movements of in and outflow. During spring tide the transports increase and during neap tide stay more or less the same, with a net sediment transport directed offshore.

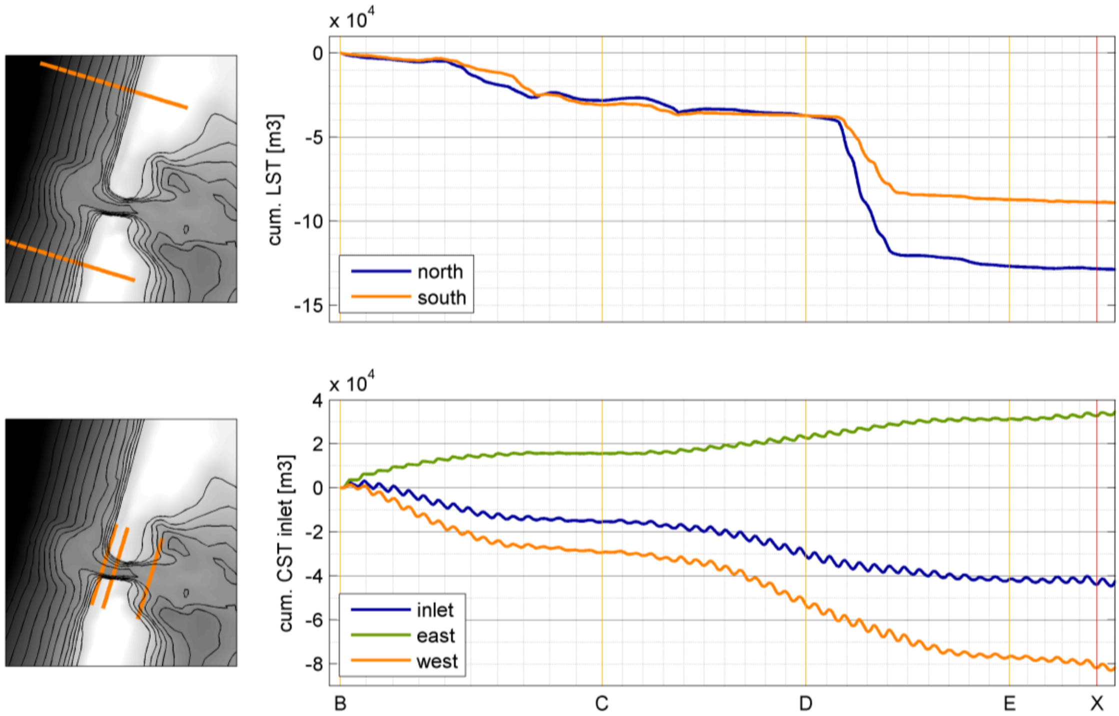

Figure 5.6 – LST, positive is northward directed (top) and CST, positive is onshore directed (bottom), location of the cross-sections (left)

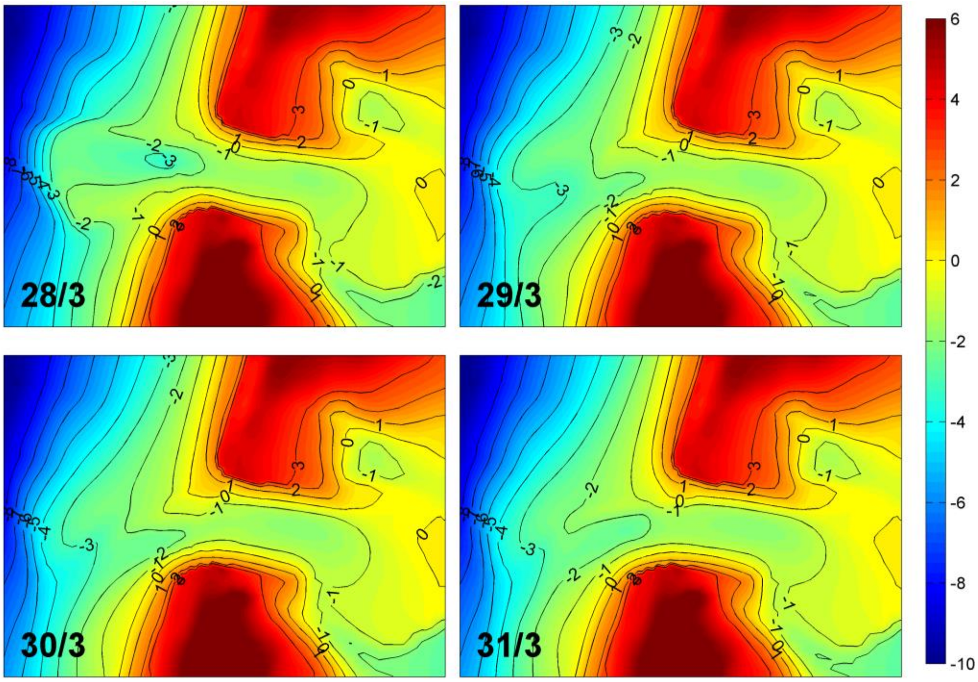

Figure 5.7 - Spit formation during spring tide (just after stage D) and during high wave conditions causing large LST

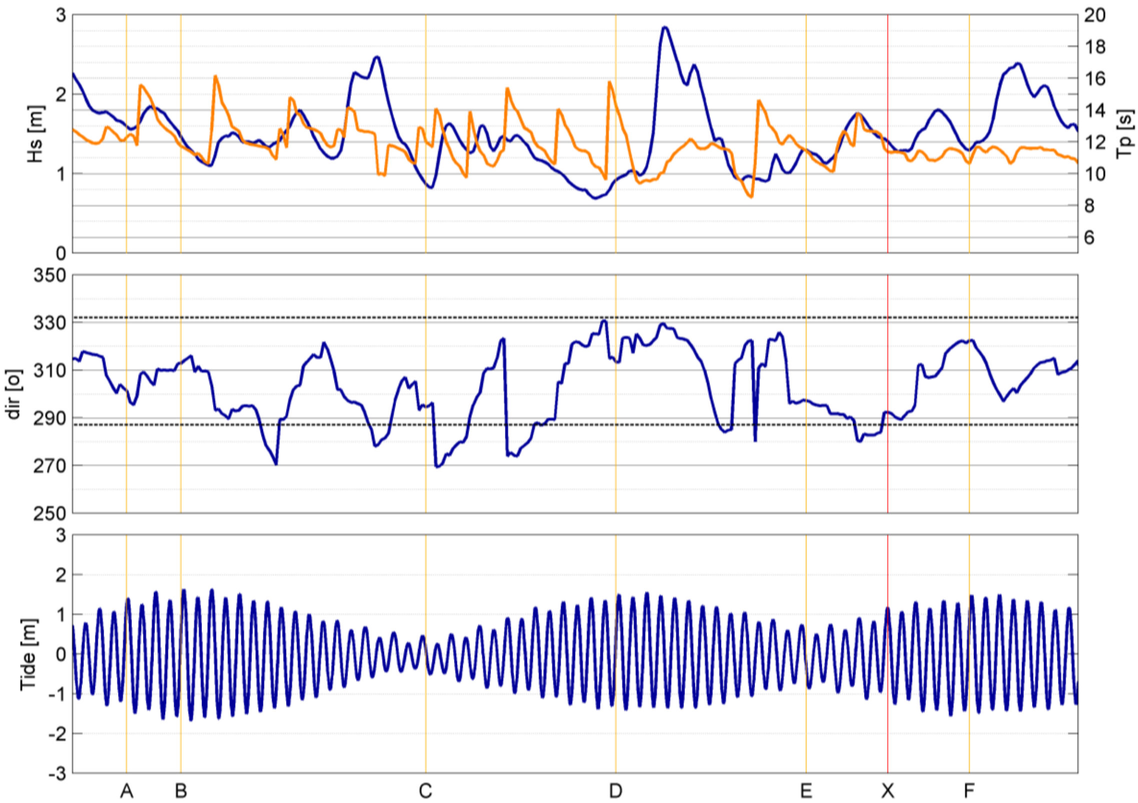

Figure 5.8 - Wave height and period (top); wave direction (middle) with indication of wave angle of incidence perpendicular on on the coast (287degrees) and wave angle of incidence corresponding to maximum LST (45 degrees); tide (bottom).Yellow lines indicate the different stages and X (red line) corresponds to the moment of inlet closure.

5.3 Long waves

According to Nahon et al. (2011) long waves may be important in the onshore sediment transports and in closure of the inlet. Therefore simulations with and without long waves are performed in order to investigate the influence of the long waves.

Comparing both simulations with and without long waves, the following results are obtained. Small differences are visible in the bathymetry results (Appendix Figure E.2), therefore a plot with the difference in bathymetry is shown in Figure 5.9. The blue colour corresponds to erosion due to long waves (compared to stationary waves) and red colour corresponds to accretion due to long waves (compared to stationary waves). Along the coast, the long waves have an eroding effect during the total period. In stage C little accretion effect south of the spit is noticeable, while in D some erosion effects south of the formed ebb delta can be seen and accretion effects north of the ebb delta. This effect is also visible in stage E; north of the spit the shoal is shallower in case of long waves. Besides, the spit is extending due to long waves.

Based on the differences in the bathymetry, it suggests long waves cause some erosion along the coast, but are forming a more pronounced spit.

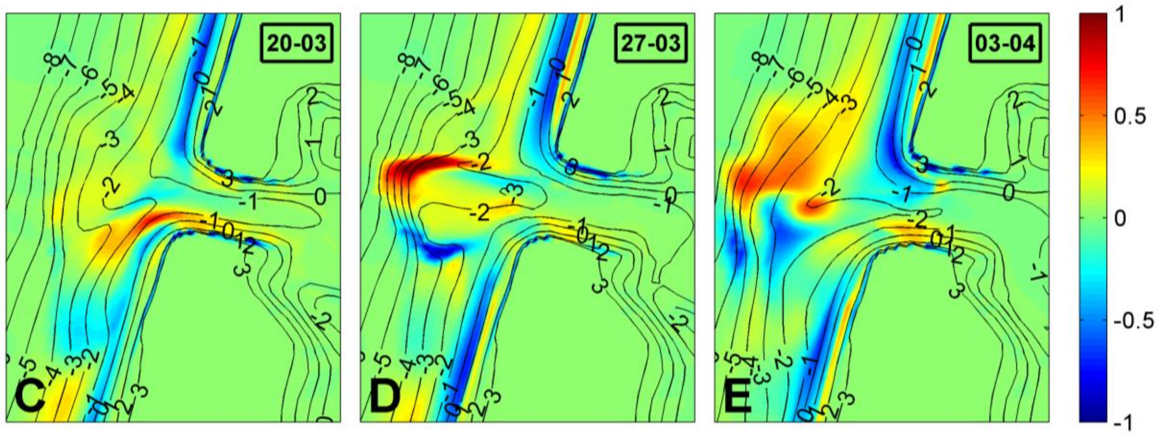

Figure 5.9 - Difference in bathymetry [m], contourlines correspond to the bathymetry with the long waves.

The differences in the sediment transports are only significant for the LST. The cross-shore transports are comparable for both simulations (Appendix Figure E.3). In Figure 5.10 the longshore transports corresponding with the long waves and without the long waves are shown for cross-sections north and south of the inlet[5]. Both net transports are directed southward and the trend is comparable. Based on Figure 5.10, longshore transports seem to be influenced by the long waves, resulting in less LST.

[5] Location of the cross-sections is the same as shown in Figure 5.6.

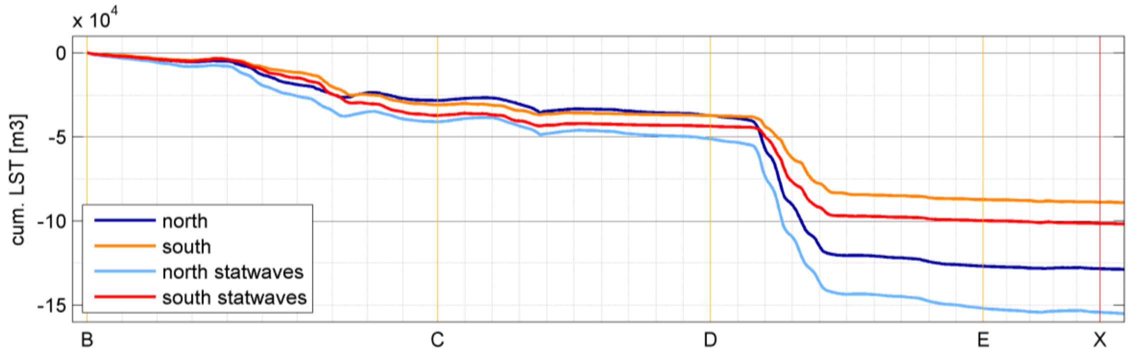

Figure 5.10 - LST of cross-section north and south in the inlet for long waves and stationary waves

For several points, in line with the inlet, the wave heights are shown. The location of these points can be seen in Figure 5.12 and the wave height of the long waves, short waves and the total wave height for the points 4-7 are shown in Figure 5.11 (point 1-3 is shown in Appendix Figure E.4).

Comparing the long waves with the short waves and the total wave height, there is hardly any difference visible between the short wave height and the total wave height. Only during higher wave conditions (around March 18th), the total wave height is slightly larger during ebb. For the wave height in point 6 and 7 (around March 17th and March 18th) the total wave height is 10-20 cm larger than the short wave height, which is an increase of 10-15%.

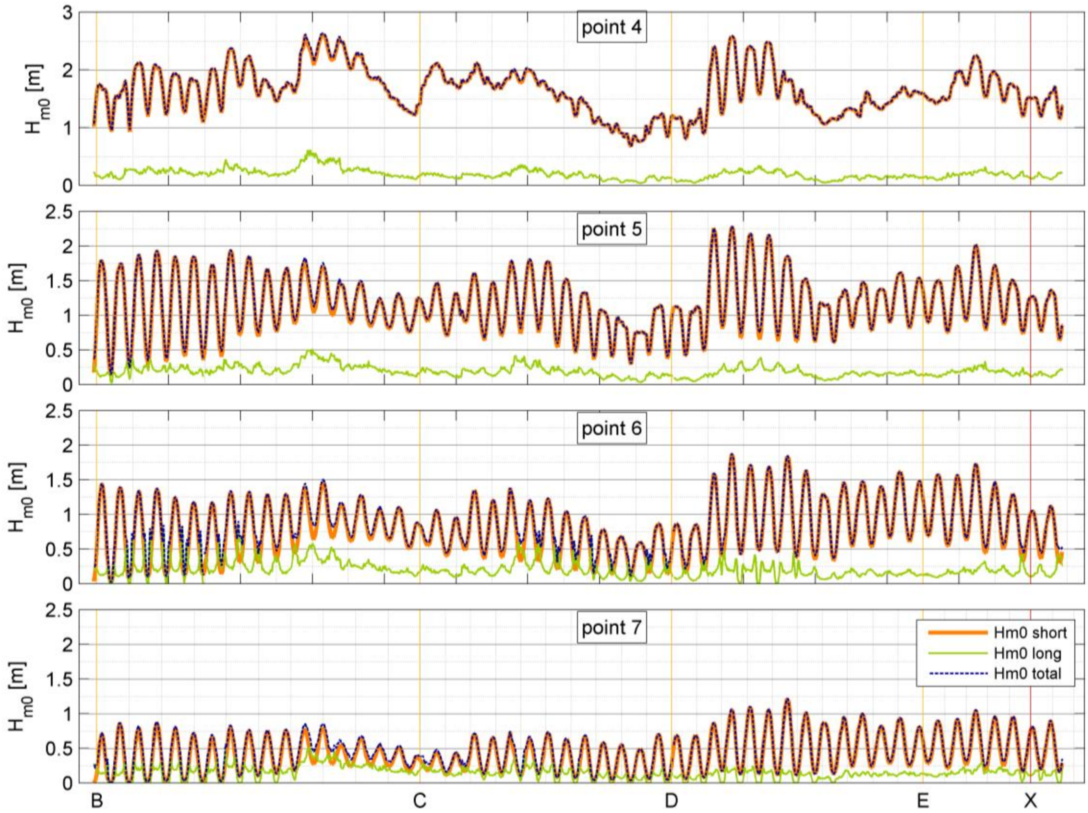

Figure 5.11 - Wave heights for point 4-7; long waves, short waves and total wave height.

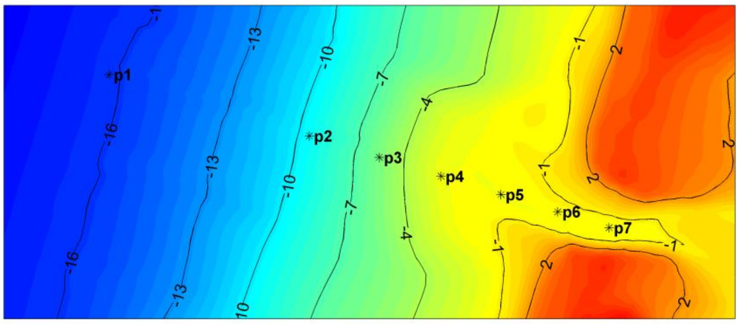

Figure 5.12 – Location of points

5.4 Current feedback on wave propagation

Cross-shore sediment transports may be influenced by the current feedback on the waves, according to Nahon et al. (2011). In XBeach this process can be turned on or off with the 'wave current interaction'-parameter (wci). In this section the results of simulations with the wci-parameter turned on and off are compared.

Turning the parameter 'wave current interaction' (wci) on, means that the Lagrangian velocities are taken into account in the wave action propagation speeds in x- and y-direction. Besides the current refraction terms in the propagation speed in θ-space is taken into account (Roelvink et al., 2010). According to Dodet et al. (2013) taking into account this process, there will be more onshore directed sediment transport than without this process in case of shallow tidal inlets. In Figure 5.13 the bathymetry of the simulations is shown; 'wci'-parameter turned on (up) and 'wci'-parameter turned off (bottom).

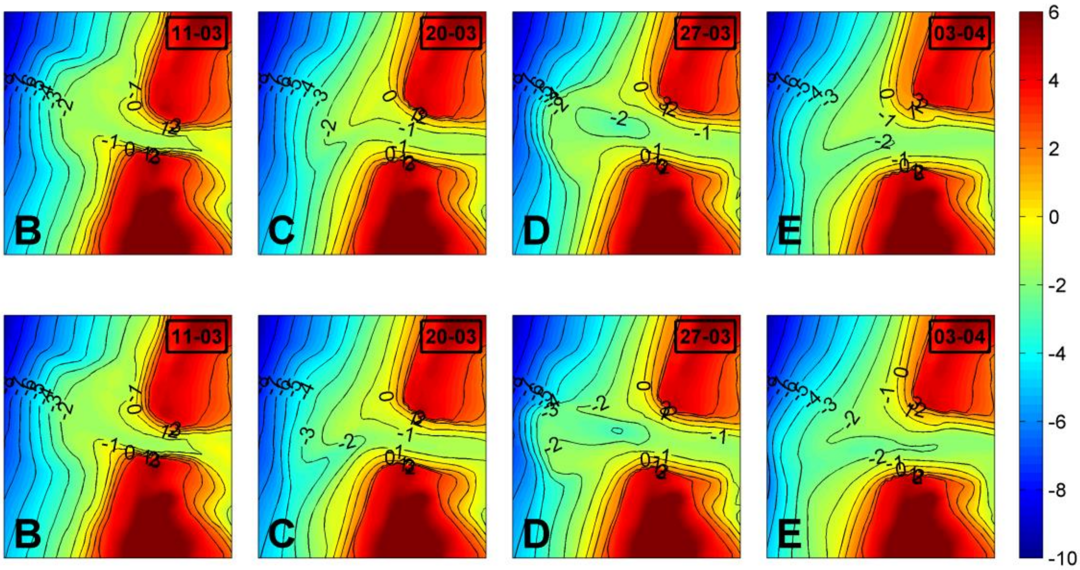

Figure 5.13 - Bathymetry inlet [m] MSL; 'wci' turned on (up) and 'wci' turned off (bottom)

When the 'wci'-parameter is turned on, the spit formation is larger (i.e. a larger area has a depth of -1 m at the location of the spit) during the first period. Besides, the ebb delta has slightly moved onshore compared to the ebb delta in case of not taken into account the current feedback on the wave propagation. During the next period to D, a more pronounced ebb delta has developed. In stage E a spit is formed again, which is larger in case of feedback on wave propagation. Besides the inlet channel is shallower than in case of turning off the ‘wci’-parameter. It seems the offshore transport is less when the ‘wci’-parameter is turned on. This slightly less offshore transport is shown in Figure 5.14, where the CST is plotted for two cross-sections (location of these are the same as shown in Figure 5.6). The net transport is still offshore directed, but has reduced with about 20% in case of the cross-section in the middle of the inlet and about 10% in case of the cross-section at the mouth of the inlet.

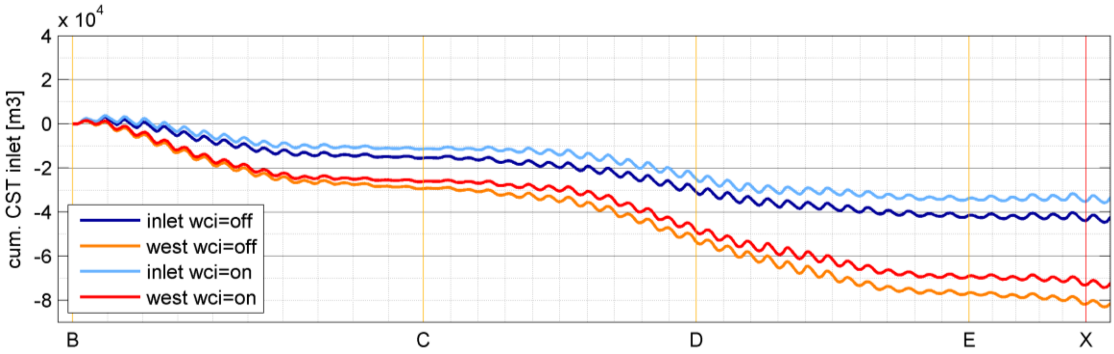

Figure 5.14 - CST of cross-sections in the middle of the inlet and west of the inlet for 'wci'-parameter turned on and off.

Based on these results, the current feedback on the waves causes less offshore transport and causes a more pronounced spit.

CHAPTER 6

Conclusions & Recommendations

6.1 Conclusions

The main objective of this study was to *understand the physical processes involved in closure of the artificially breached inlet of the Santo André Lagoon*. To achieve this objective, research questions were formulated and answered in this study:

- How does the system develop?
- Which processes are involved in the morphological development?
- What is the influence of the physical processes that were not taken into account in previous modelling?

Therefore analysis of the measured data was performed to understand the morphological development of the system and the contribution of the absent (in previous modelling) processes to the development of the system were investigated. Resulting in the conclusions and recommendations described in the next sections.

Morphological development of the system

Strong currents are flowing through the inlet, stronger bottomfriction is necessary to obtain corresponding water levels. This stronger bottomfriction is too strong for the shore adjacent to the inlet. It leads to decreasing of velocity that is inducing an unrealistic decrease of the longshore transports. Using spatial varying bottomfriction, the modelling results of the morphological development of the inlet correspond better to the measured data.

The ebb delta formed after breaching of the inlet is still visible in the model and the formation of the spit is too small comparing to the observations. This suggests an underestimation of the onshore sediment transports, by physical processes. It may be underestimation of the effect of these processes, but the absence of some physical process descriptions in XBeach that influence the onshore transports may be a reason as well. Nahon et al. (2011) suggested transports in the swash zone were not included in the model and may be important in the onshore transports. However, this is not investigated in this study.

Not only underestimating or the absence of physical process descriptions in XBeach resulting in onshore sediment transports may be the reason of modelling the development of the ebb delta and spit not correctly. The tide seems to be dominant in erosion of the inlet and is hindering a spit formation. High velocities occur of which the ebb currents are dominant, reaching velocities of 3 m/s (during spring tide). Eroded sediment from the inlet and spit is flushed out and contributes to preserving the ebb delta. Besides, these strong currents may hinder the onshore directed transports and the formation of a spit. Measurements of the inlet velocities are only performed during the first 26 hours after breaching (Pires et al., 2011) in which velocities of 2 m/s occur at the end of this short period. This suggests the tide and the accompanied velocities are overestimated by the model. The cross-sectional area of the inlet is larger in the model than in the observations and may be a reason for these high velocities.

During neap tide when the current velocities are smaller the spit is formed. The spit is also formed when large longshore transports occur. The largest transports occur for waves propagating towards the coast with an angle of incidence of about 45°. In this study the largest longshore transports occur when large waves (Hs > 2m) propagating towards the coast with an angle of incidence of about 45-60°, resulting in spit formation during spring tide. This suggests longshore transports (caused by large waves, Hs > 2m) are important in forming of a spit and thus in closure of the inlet. The sediment is transported by the alongshore currents and is 'pushed' onshore by the strong onshore currents during flood.

Influence of processes – absent in previous modelling

The contribution of the physical processes that were absent in previous modelling are investigated: wave asymmetry, long waves and current feedback on the waves. Resulting in better agreement with observations:

- Although this process is not investigated for the development of the inlet, it is investigated and used for the calibration part of this study. According to this, the following can be concluded. Increasing wave asymmetry causes more onshore transport (i.e. increasing the wave asymmetry factor in XBeach causes onshore transport). This results in accretion of the coast and closing of the inlet in this model (i.e. moving the ebb delta onshore and transforming into a berm that closes the inlet).
- The long waves occurring at the Santo André coast are relatively small, compared to the short waves. Comparing results, a spit is slightly better formed when the contribution of the long waves was included in the model. Therefore long waves do influence the morphological development, resulting in a better spit formation.
- Current feedback on the wave propagation (i.e. the wave action propagation speed is influenced by the current velocities and the current refraction is taken into account) cause less offshore transport and better forming of a spit. Therefore the contribution of the current feedback on the wave propagation is improving the morphological development of the inlet according to the measurements in this study.

Although the inlet is not closing in the model, understanding of the processes involved in the morphological development and closure has improved. Wave asymmetry, long waves and current feedback on the waves influence the onshore transport and spit formation, which could lead to closure of the inlet in the end. But the onshore transport is underestimated in the model and important processes causing onshore transport may be absent. Swash may be a missing process to result in more onshore transports in this model. On the other hand, tide seems to be overestimated. Large velocities occur in the inlet, resulting in strong outflow, forming ebb delta and eroding the spit. This may be a caused by the cross-sectional area of the inlet, which is larger in depth in the model than in the observations.

6.2 Recommendations

Based on the results and conclusions some recommendations for further research on this study can be made, and some remarks in order to improve XBeach.

General

According to the available data there are some remarks to be made. The bathymetry data of the several stages are containing inaccuracies at every location, where the resolution has its limitations. For the total area the same bathymetry dataset is used, only the inlet with its ebb delta and spit, channel and flood delta are measured every stage.

Wave and tidal data are obtained from regional models, although the RMSE of these models is of about 10%, there are some uncertainties in the wave and tidal forcing.

With these uncertainties, more accurate measurements for bathymetry, wave and tide are preferred. Besides, more data to calibrate the model could improve the model results and the understanding of the morphological behaviour. Measurements such as longshore transport, cross-shore transport and more accurate velocities during a longer period may improve the model calibration.

In order to see if the processes involved in the morphological development are comparable every year, different datasets of different opening periods need to be collected and used in the model.

Onshore directed transports are underestimated or missing. Although many parameters have been used in XBeach to increase the onshore transports, there are still some possibilities to improve the model and its results. A process described in Nahon et al. (2011) that contribute to the onshore transports is short wave swash. Further investigation on these processes is recommended.

Further research is recommended to comparable shallow inlets to investigate if the same processes resulting in comparable morphological development. Or the behaviour of the inlet of the Santo André Lagoon may be completely unique.

Using another morphological model may give more insight in the physical processes involved. XBeach is a storm impact model and is not primarily designed for these kinds of morphological developments. So it has its drawbacks, less validated processes and strong eroding behaviour associated with the development of the coast. Besides, the choice for XBeach is based on the missing processes of long waves. The influence of the long waves in this study and this model is not significant large, therefore a model such as Delft3D may give more comparable results according to the measured data or give more insight in the influence of other physical processes.

XBeach

Spatial varying bottomfriction improved the results significantly, but it uses one value for every depth. The bottom is changing, so the bottomfriction should be changing as well. In XBeach the formulation of White-Colebrook is implemented, which calculates the bottomfriction based on the depth, but is underestimating the bottomfriction. Improvement for this formulation could be useful for the right calculation of the bottomfriction.

Using spatial varying bottomfriction with Chézy values and the Chézy formulation, there can be some improvement as well. In this study two different values were used for which a transition zone was necessary to prevent strange scouring holes in the bathymetry. Optimising this formulation and function, could reduce the transition zone and ending up in better results according to bottomfriction.

In this study source problems were encountered when using XBeach with several processors. The simulations stopped without giving any errors. To use several processors, XBeach divides the model in several domains. In this study it is found the borders of these domains may be of importance in successfully calculation of the simulation. Some processes, e.g. avalanching, are not calculated over the borders of the domains. In case of avalanching, the results show strange bumps in the bathymetry. Simulations where the border of the domain was on the same location as the shoreline, it showed these kinds of numerical 'problems' or the simulation just stopped. Using a division where the shoreline is not on the same location, calculation was successful, but limited processors could be used.

References

Bertin, X., Bruneau, N., Breilh, J.-F., Fortunato, A. B., & Karpytchev, M. (2012). Importance of wave age and resonance in storm surges: The case Xynthia, Bay of Biscay. *Ocean Modelling, 42*, 16-30. doi: 10.1016/j.ocemod.2011.11.001

Bertin, X., Fortunato, A. B., & Oliveira, A. (2009a). A modeling-based analysis of processes driving wave-dominated inlets. *Continental Shelf Research, 29*(5-6), 819-834. doi: 10.1016/j.csr.2008.12.019

Bertin, X., Fortunato, A. B., & Oliveira, A. (2009c). Morphodynamic Modeling of the Ancão Inlet, South Portugal. *Journal of Coastal Research*(SI 56), 10-14.

Bezerra, M., Ferreira, Ó., Pacheco, A., Freitas, M. d. C., Pires, R., Andrade, C., & Taborda, R. (2011). Stages in the evolution of an ephemeral tidal inlet immediatly after artioficial opening. *Journal of Coastal Research*(SI 64), 1453-1456.

Boothroyd, J. C., Friedrich, N. E., & McGinn, S. R. (1985). Geology of microtidal coastal lagoons: Rhode Island. *Marine Geology, 63*, 35-76.

Bosboom, J., & Stive, M. J. F. (2012). *Coastal Dynamics 1*. Delft: VSSD.

Carman, P. C. (1937). Fluid through granular beds. *Transactions, Institution of Chemical Engineers, 15*, 4-20.

Chawla, A., & Kirby, J. T. (2002). Monochromatic and random wave breaking at blocking points. *Journal of Geophysical Research, 107*(C7). doi: 10.1029/2001JC001042

Correia, M. J., Costa, J. L., Chainho, P., Félix, P. M., Chaves, M. L., Medeiros, J. P., . . . Cancela da Fonseca, L. (2012). Inter-annual variations of macrobenthic communities over three decades in a land-locked coastal lagoon (Santo André, SW Portugal). *Estuarine, Coastal and Shelf Science, 110*, 168-175. doi: 10.1016/j.ecss.2012.04.028

Costa, M., Silva, R., & Vitorino, J. (2001). Contribuição para o estudo do clima de agitação marítima na costa Portuguesa. . *2as Jornadas de Eng. Cost. e Port.*, AIPCN, 20p.

Cruces, A. (2014). [Personal communication].

Cruces, A., Freitas, M. C., & Andrade, C. (2009). *Morphodynamics of the artificial inlet of Santo Andre coastal lagoon (SW Portugal) - twelve years of monitoring*. Paper presented at the 6th Symposium on the Atlantic Iberian Margin.

Cruces, A., Freitas, M. C., Andrade, C., Munhá, J., Tassinari, C., Vale, C., & Jouanneau, J.-M. (2006). The importance of geochemistry in multidisciplinary studies of lagoonal environments at different time scales: the case of Santo André Lagoon (SW Portugal). *Journal of Coastal Research*(SI 39), 1716-1722.

Dodet, G. (2013). *Morphodynamic modelling of a wave-dominated tidal inlet: the Albufeira Lagoon.* (PhD Thesis), L'Université de La Rochelle, La Rochelle.

Dodet, G., Bertin, X., Bruneau, N., Fortunato, A. B., Nahon, A., & Roland, A. (2013). Wave-current interactions in a wave-dominated tidal inlet. *Journal of Geophysical Research: Oceans, 118*(3), 1587-1605. doi: 10.1002/jgrc.20146

Dodet, G., Bertin, X., & Taborda, R. (2010). Wave climate variability in the North-East Atlantic Ocean over the last six decades. *Ocean Modelling, 31*(3-4), 120-131. doi: 10.1016/j.ocemod.2009.10.010

Fortunato, A. B., Pinto, L., Oliveira, A., & Ferreira, J. S. (2002). Tidally generated shelf waves off the western Iberian coast. *Continental Shelf Research, 22*, 1935-1950.

Freitas, M. d. C., Andrade, C., Rocha, F., Tassinari, C., Munhá, J. M., Cruces, A., . . . Marques da Silva, C. (2003). Lateglacial and Holocene environmental changes in Portugese coastal lagoons 1: the sedimentological and geochemical records of the Santo André coastal area. *The Holocene, 13,3*, 433-446.

Grasso, F., Michallet, H., & Barthélemy, E. (2011). Sediment transport associated with morphological beach changes forced by irregular asymmetric, skewed waves. *Journal of Geophysical Research, 116*(C3). doi: 10.1029/2010jc006550

Hazen, A. (1911). Discussion: dams on sand foundations: transactions. *American Society of Civil Engineering, 73*, 199.

Hegge, B. J. (1994). *Low-energy sandy beaches of southwestern Australia: Two-dimensional morphology and dynamics.* (PhD Thesis), University of Western Australia, Perth (unpublished).

Hoefel, F., & Elgar, S. (2003). Wave-induced sediment transport and sandbar migration. *Science, 299*(5614), 1885-1887. doi: 10.1126/science.1081448

Holthuijsen, L. H. (2007). *Waves in Oceanic and Coastal Waters*. New York, United States of America: Cambridge University Press.

Jarrett, J. T. (1976). Tidal prism - inlet area relationships. *GITI Report*. Vicksburg, Mississippi: US Army Engineer Waterways Experiment Station.

Kozeny, J. (1927). Ueber kapillare Leitung des Wassers im Boden. *Sitzungsberichte der Akademie der Wissenschaften in Wien, 136*, 271-306.

Krumbein, W. C., & Monk, G. D. (1942). Permeability as a function of the size parameters of unconsolidated sand. *Transactions of the American Institute of Mining and Metallurgical Engineering, h73*, 199.

Longuet-Higgins, M. S., & Stewart, R. W. (1962). Radiation stress and mass transport in gravity waves, with application to 'surf beats'.

Masselink, G., & Li, L. (2001). The role of swash infiltration in determining the beachface gradient a numerical study. *Marine Geology, 176*, 139-156.

McCall, R. T., Van Thiel de Vries, J. S. M., Plant, N. G., Van Dongeren, A. R., Roelvink, J. A., Thompson, D. M., & Reniers, A. J. H. M. (2010). Two-dimensional time dependent hurricane overwash and erosion modeling at Santa Rosa Island. *Coastal Engineering, 57*(7), 668-683. doi: 10.1016/j.coastaleng.2010.02.006

Nahon, A., Fortunato, A. B., Bertin, X., Pires, A. R., Oliveira, A., Freitas, M. C., & Andrade, C. (2011). Modelação numérica da abertura e fecho de uma embocadura artificial (Lagoa de Santo André, Portugal). *Revista de Gestão Costeira Integrada, 11*(3), 341-353. doi: 10.5894/rgci260

O'Brien, M. P. (1969). Equilibrium flow areas of inlets on sandy coasts. *Journal of the Waterway and Harbors Division, Proceedings of the American Society of Civil Engineers*, 43-52.

Pires, A. R., Freitas, M. d. C., Andrade, C., Taborda, R., Ramos, R., Pacheco, A., . . . Cruces, A. (2011). Morphodynamics of an ephemeral tidal inlet during a life cycle (Santo André Lagoon, SW Portugal). *Journal of Coastal Research*(SI 64), 1565-1569.

Ranasinghe, R., & Pattiaratchi, C. (2000). Tidal inlet velocity asymmetry in diurnal regimes. *Continental Shelf Research, 20*, 2347-2366.

Roelvink, D., Reniers, A., van Dongeren, A., van Thiel de Vries, J., Lescinski, J., & McCall, R. (2010). XBeach Model Description and Manual. *June 21, 2010*(version 6).

Roelvink, D., Reniers, A., van Dongeren, A., van Thiel de Vries, J., McCall, R., & Lescinski, J. (2009). Modelling storm impacts on beaches, dunes and barrier islands. *Coastal Engineering, 56*(11-12), 1133-1152. doi: 10.1016/j.coastaleng.2009.08.006

Ruessink, B. G., van den Berg, T. J. J., & van Rijn, L. C. (2009). Modeling sediment transport beneath skewed asymmetric waves above a plane bed. *Journal of Geophysical Research, 114*(C11). doi: 10.1029/2009jc005416

Sallenger, A. (2000). Storm impact scale for barrier islands. *Journal of Coastal Research, 16*(3), 890-895.

Seabergh, W. (2006). *Coastal Engineering Manual (EM, 1110-2-1100)* (Vol. Part II - Chapter 6, "Hydrodynamics of Tidal Inlets"): U.S. Army Corps of Engineers.

Silveira, M., Encarnação, P., Vidal, A., & Cancela da Fonseca, L. (2009). Aves aquaticas e gestao da Lagoa de Santo Andre. *Journal of Integrated Coastal Zone Management, 9*(3), 55-70.

Soulsby, R. L. (1997). *Dynamics of Marine Sands: a manual for practical applications*. London: Thomas Telford Publications.

Steenhauer, K. (2010). *An experimental and numerical study of surface-subsurface interaction for bore-driven swash on coarse-grained beaches.* (Phd Thesis), School of Engineering, University of Aberdeen, Aberdeen.

Van de Kreeke, J. (1992). Stability of Tidal Inlets; Escoffier's Analysis. *Shore and Beach, 60*(1), 9-12.

Van de Kreeke, J. (2004). Equilibrium and cross-sectional stability of tidal inlets: application to the Frisian Inlet before and after basin reduction. *Coastal Engineering, 51*(5-6), 337-350. doi: 10.1016/j.coastaleng.2004.05.002

Van Rooijen, A. A. (2011). *Modelling Sediment Transport in the Swash Zone.* (MSc Thesis), Delft University of Technology, Delft.

Van Thiel de Vries, J. S. M. (2009). *Dune erosion during storm surges.* (Phd Thesis), Delft University of Technology, Delft.